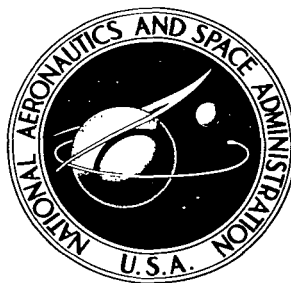


NASA TECHNICAL NOTE



NASA TN D-2130

C.1

LOAN COPY: R
AFWL (W
KIRTLAND AFI

0154397



TECH LIBRARY KAFB, NM

NASA TN D-2130

**EFFECTIVENESS OF RADIATION SHIELDS
FOR THERMAL CONTROL OF VEHICLES
ON THE SUNLIT SIDE OF THE MOON**

by John C. Arvesen and Frank M. Hamaker

Ames Research Center

Moffett Field, Calif.

EFFECTIVENESS OF RADIATION SHIELDS FOR THERMAL CONTROL
OF VEHICLES ON THE SUNLIT SIDE OF THE MOON

By John C. Arvesen and Frank M. Hamaker

Ames Research Center
Moffett Field, Calif.

NATIONAL AERONAUTICS AND SPACE ADMINISTRATION

For sale by the Office of Technical Services, Department of Commerce,
Washington D.C. 20230 -- Price \$1.25



0154397

EFFECTIVENESS OF RADIATION SHIELDS FOR THERMAL CONTROL

OF VEHICLES ON THE SUNLIT SIDE OF THE MOON

By John C. Arvesen and Frank M. Hamaker

SUMMARY

Analyses are presented for studying the problems of thermal control associated with vehicles on the lunar surface during the daytime and evaluating the effectiveness of solar and lunar radiation shields in minimizing these problems. Included in the analyses are inputs of direct solar radiation, solar radiation reflected from the lunar surface, radiation emitted from the lunar surface, internally generated power, and, for a shielded vehicle, radiation reflected and emitted from the shields. An additional analysis is presented for studying the effect of conduction in the skin upon the temperature variation around a vehicle illuminated from the side.

Temperatures of unshielded vehicles were found to be a strong function of the ratio of solar absorptance to emittance (α_s/ϵ) of their surfaces and might be excessively high during daytime. Even with coatings of very low α_s/ϵ , the vehicle temperatures could be undesirably high as a result of absorption of radiation emitted from the hot lunar surface. When an unshielded vehicle is subjected to solar illumination from the side, as may be encountered at dawn, dusk, or at the poles, large temperature differences and gradients are found to occur from the sunlit to the shaded side of the vehicle.

Results of this study indicate that solar and lunar radiation shields can eliminate many of the thermal problems apparent with unshielded vehicles on the lunar surface. Solar shields may reduce the amount of incident solar radiation so greatly that the temperatures on the vehicle will become independent of the vehicle's surface properties. Lunar radiation shields may be used to isolate, effectively, the vehicle from radiation emitted from the lunar surface. With a combination of solar and lunar shields, the surface temperatures of a vehicle can be reduced to a desirable level.

INTRODUCTION

Thermal control of a vehicle on the surface of the moon is complicated by the extremes in temperature and incident radiation encountered. The surface temperature reaches 240°F or more at the subsolar point and, during lunar night, drops to -240°F or lower (see ref. 1). The absence of an atmosphere to attenuate or diffuse direct solar radiation causes an extremely large difference in temperature of sunlit and shadowed lunar areas. In this environment, vehicles would be expected to provide thermal protection for both men and equipment.

With the lunar temperature and incident solar radiation varying over such wide ranges during the day, the problem of maintaining the temperature of the interior of a vehicle within required limits, say 60° F to 90° F, may be very difficult. If the outside surface temperature of the vehicle is much different from the interior temperature, a substantial weight of insulation may be required to adequately reduce the rate of heat flow into or out of the vehicle. Thus, for lunar vehicles, it is reasonable to assume a design goal of maintaining skin temperature at approximately the same level as is desired in the interior. A study of the temperatures of the exterior of a lunar vehicle and the parameters which affect these temperatures, therefore, becomes meaningful in terms of achieving desired thermal control.

One method of reducing the maximum vehicle temperature is by the use of coatings with very low ratios of solar absorptance to thermal emittance. However, even with such coatings, the radiation from the hot lunar surface may still cause undesirably high temperatures. Furthermore, such coatings may possibly be susceptible to degradation of radiative properties due to environment exposure (ref. 2.).

Another method of thermal control of lunar vehicles is the use of external radiation shields. Solar radiation shields have been shown to be very effective for thermal protection of a solar probe (ref. 3) where the incident radiation intensity varied by two orders of magnitude. Stevenson and Grafton (ref. 4) studied the effect of a solar shield upon the temperatures of objects on the lunar surface at the subsolar point. Because the objects studied were still directly exposed to the hot lunar surface, the shield was not adequate under all conditions to prevent excessively high temperatures of the objects.

In the present study, the concept of radiation shielding is extended to include a lunar radiation shield that isolates the vehicle from radiation emitted from the lunar surface and to evaluate the effectiveness of a combination of solar and lunar shields. An expression for the temperature distribution over the surface of unshielded vehicles on the lunar surface is developed and the thermal problems associated with a particular vehicle configuration are studied as a basis for comparison with the shielded configuration. A general analysis is also presented from which the temperatures of any shielded vehicle may be calculated. The effectiveness of solar and lunar radiation shields is then determined as a function of geometry, solar absorptance and thermal emittance properties, solar illumination angle, and internally generated heat.

NOTATION

- A surface area, sq ft
- b thickness of vehicle's skin, ft
- C thermal conductance ($C = bk$), Btu/hr-°F
- D vehicle diameter, ft

E	solar constant, $442.8 \text{ Btu/hr-ft}^2$, 129.7 watts/ft^2
F	radiation configuration factor
k	thermal conductivity, $\text{Btu-ft/hr-ft}^2 \text{ } ^\circ\text{F}$
Q	heat-transfer rate, Btu/hr
S	direct solar radiation, Btu/hr
T	temperature, $^\circ\text{R}$
X	solar-shield separation distance, ft
α_s	solar absorptance
γ	angle between the sun's direction and a normal to the lunar surface, deg
ϵ	thermal emittance
θ	angle between the sun's direction and a normal to the vehicle's surface, deg
ρ_m	lunar reflectance to solar radiation
σ	Stefan-Boltzmann constant ($0.173 \times 10^{-8} \text{ Btu/hr-ft}^2\text{-}^\circ\text{R}^4$)
ϕ	azimuth angle of a point on surface of vehicle with respect to sun, deg
ψ	orientation angle of a point on the vehicle with respect to the lunar surface (fig. 2), deg

Subscripts

d	directly incident
dA	elemental area
em	emitted from the lunar surface
im	incident upon lunar surface
m	lunar surface
r	reflected
rm	reflected from lunar surface

ss subsolar point

t total

ANALYSIS

Analyses are developed that can be used to determine the temperatures of unshielded and shielded vehicles anywhere on the lunar surface. The temperature of an elemental area on the surface of the unshielded vehicle is found by a relatively simple method that yields a closed-form solution. A more complex analysis, requiring machine computation, is then developed from which temperatures of areas of the surface of a shielded vehicle may be calculated.

A list of general assumptions applicable to both analyses is presented to define their limits of applicability. Based upon these assumptions, a heat balance is made for an area on the surface of the vehicle. The heat balance includes inputs of direct solar radiation, solar radiation reflected from the lunar surface, radiation emitted from the lunar surface, internally generated heat, and, for a shielded vehicle, radiation reflected and emitted from the shields. The equilibrium temperature of the area may then be calculated by equating total heat input to total heat radiated from the area.

A heat-transfer analysis is also developed to study the effect of conduction in the skin upon the temperature variation around a vehicle illuminated from the side.

General Assumptions

As the radiative heat-transfer analyses associated with unshielded and shielded vehicles on the lunar surface are developed, a number of assumptions or approximations are introduced. For clarity, these are collected in the following list:

Lunar Environment:

1. The temperature of the lunar surface at the subsolar point is 240° F.
2. The temperature of the lunar surface on the dark side is -240° F.
3. The thermal conductivity of the lunar surface is negligible.
4. The spatial environment is considered to be a radiation sink at -460° F (0° absolute).
5. The lunar surface emits and reflects radiation diffusely in accordance with Lambert's law.
6. The reflectance of the lunar surface is the same over the entire surface.
7. The lunar surface in the immediate vicinity of the vehicle may be analytically approximated by an infinite flat plane of uniform temperature.
8. Thermal effects of radiation from the earth are negligible.

Vehicle:

1. The surface of the vehicle reflects and emits radiation diffusely in accordance with Lambert's law.
2. The absorptance of the surface of the vehicle to infrared radiation is equal to its emittance (i.e., exhibits gray-body characteristics in the infrared region).
3. Radiation that is reflected or emitted from the vehicle does not return to its surface (except as indicated for the radiation-shield analysis).
4. The thermal conductance of the skin of the vehicle is considered to be zero unless otherwise specified.
5. The temperature of the surface of the vehicle is assumed to be that reached at equilibrium.
6. No heat is lost from the surface of a vehicle by conduction or radiation into or through the vehicle.
7. No heat is conducted into the vehicle from the lunar surface or vice versa. (The vehicle is on a nonconducting base.)
8. The shadow cast upon the lunar surface by the vehicle has a negligible effect upon vehicle temperatures. (However, the effect of the shadow cast by the solar shield is included.)

Shields:

1. The shields are considered to have isothermal surfaces.
2. The shields emit and reflect radiation diffusely in accordance with Lambert's law.

Lunar Thermal Environment

An evaluation is made of solar radiation incident upon and the total radiation leaving an area of the lunar surface. Lunar surface temperatures are discussed and a simple approximation to the temperature at any point on the lunar surface is given.

Incident solar radiation. - The direct solar radiation incident upon an elemental area dA_m of the lunar surface depends only upon the angle of illumination. If the angle between the sun's direction and a normal to the lunar surface is defined as γ , the direct solar radiation is

$$dS_{im} = E \cos \gamma \, dA_m \quad 0 \leq \gamma \leq \pi/2 \quad (1)$$

where E is the value of the solar constant.

Reflected solar radiation.- The solar radiation reflected from the lunar surface is

$$dS_{rm} = \rho_m E \cos \gamma \, dA_m \quad (2)$$

where ρ_m is the fraction of solar radiation reflected.

Emitted lunar radiation.- The radiation emitted from an elemental area of the lunar surface may be determined from the Stefan-Boltzmann law as

$$dQ_{em} = \sigma T_m^4 \, dA_m \quad (3)$$

since the emittance of the lunar surface has been determined by Pettit and Nicholson (ref. 5) to be very nearly unity.

Lunar surface temperatures.- William M. Sinton and associates at Lowell Observatory (refs. 1 and 6) have measured lunar surface temperatures using modern infrared techniques. They have determined the "mean spherically emitting" subsolar point temperature to be 389°K (240°F) and the dark side "midnight" temperature to be $122^\circ \text{K} \pm 3^\circ \text{K}$ ($-240^\circ \text{F} \pm 5^\circ \text{F}$). In addition, they have constructed isothermal maps of the lunar surface at various phase angles (ref. 7) from which the temperature of a point may be determined at various times during the lunar day. Typical measured temperatures are shown for various solar illumination angles in figure 1 for a small area near the center of the lunar disk. A theoretical curve of temperature variation of a model lunar surface obtained from reference 1 is also shown in figure 1. The value of conductivity used for calculating this curve is so low that it is representative of a powder or dust in a high vacuum (ref. 1). By an analysis of the temperature-time history of a lunar eclipse (refs. 8 and 9) the lunar surface has further been shown to be an extremely poor heat conductor.

If the thermal inertia of the lunar surface is assumed zero, the temperature of any area of the lunar surface will vary between the subsolar point temperature (240°F) and the dark side temperature (-240°F) as the fourth root of the cosine of the illumination angle:

$$\left. \begin{aligned} T_m &= T_{ss} \cos^{1/4} \gamma \\ T_m &= 220^\circ \text{R} \, (-240^\circ \text{F}) \end{aligned} \right\} \text{whichever is higher} \quad (4)$$

Equation (4) is also plotted in figure 1 and it is seen that the agreement of this simple expression with the measured temperature points is fairly good.

Temperature Distribution Over the Surface of an Unshielded Vehicle

The magnitude of the components of solar radiation and lunar radiation incident upon an elemental area on the surface of an unshielded vehicle are determined. A heat balance is made that includes inputs of absorbed incident

radiation and heat generated within the vehicle. From this heat balance and the Stefan-Boltzmann law, the temperature distribution over the surface of the vehicle at equilibrium may be calculated. Since the rate of change of the lunar environment is relatively low (1 lunar day \approx 29-1/2 earth days), it is felt that the assumption of equilibrium temperatures is valid unless the vehicle's skin has an unusually high thermal capacitance.

Direct and reflected solar radiation incident upon an elemental area on the vehicle.- If θ is defined as the angle between the sun's direction and a normal to an elemental area dA on the vehicle's surface, the solar radiation that is directly incident is

$$dS_d = E \cos \theta \, dA \quad 0 \leq \theta \leq \pi/2 \quad (5)$$

Reflected solar radiation incident upon the elemental area depends upon radiation reflected from the lunar surface and the integrated radiation configuration factor between the area and the entire lunar surface. Calculation of this factor involves simplifying assumptions as to the characteristics of the lunar surface, namely, that the surface is diffuse and may be approximated by an infinite flat plane (see ref. 10). The configuration factor between an arbitrarily oriented elemental area and an infinite plane is developed in reference 11 and the result may be expressed as

$$F_{dA-m} = \cos^2(\psi/2) \quad 0 \leq \psi \leq \pi \quad (6)$$

where ψ is the orientation angle with respect to the lunar surface. The radiation configuration factor is shown graphically in figure 2. The reflected solar radiation incident upon the element may now be calculated from the reciprocity relationship ($F_{dA_m-dA} \, dA_m = F_{dA-dA_m} \, dA$) and equations (2) and (6). Thus,

$$dS_r = \rho_m E \cos \gamma \cos^2(\psi/2) dA \quad (7)$$

Incident lunar radiation.- Lunar radiation incident upon the element is a function of the radiation emitted from the lunar surface (eq. (3)) and the previously calculated configuration factor (eq. (6)). It is given by

$$dQ_{im} = \sigma T_m^4 \cos^2(\psi/2) dA \quad (8)$$

Total radiation incident.- The components of solar radiation and lunar radiation may now be combined to give the following expression for the total radiation flux incident upon the elemental area:

$$dQ_t/dA = E \cos \theta + \rho_m E \cos \gamma \cos^2(\psi/2) + \sigma T_m^4 \cos^2(\psi/2) \quad (9)$$

It can be seen that the radiation incident is a function of (1) the angle of incidence of direct solar radiation on the element θ ; (2) the angle of incidence of solar radiation upon the lunar surface γ , that is, lunar latitude, longitude and time; (3) the orientation of the element with respect to the lunar surface ψ .

Heat balance on the elemental area.- The solar absorptance α_s of any surface is defined as the fraction of the total incident solar radiation that is absorbed. The absorptance of the elemental area to infrared radiation (lunar radiation) can be shown to be very nearly equal to its emittance if the vehicle's surface has fairly constant emittance properties with wavelength in the infrared region.

It is assumed, for the present, that there is no heat conducted between elements of the vehicle's skin. There can be, however, heat sources within the vehicle that will result in additional heat inputs, U , to the element. At thermal equilibrium, the total heat input to the elemental area must be equal to the heat that is radiated away. Thus,

$$\alpha_s(\text{total incident solar radiation}) + \epsilon(\text{incident lunar radiation}) + \text{internal heat} = \text{radiation emitted}$$

or

$$\alpha_s[E \cos \theta + \rho_m E \cos \gamma \cos^2(\psi/2)] + \epsilon \sigma T_m^4 \cos^2(\psi/2) + U = \epsilon \sigma T^4 \quad (10)$$

where ϵ is the emittance of the elemental area. The equilibrium temperature, T , in the absence of conduction between adjacent elements, may now be found from

$$T = \left\{ \frac{\alpha_s}{\epsilon} \left[\frac{E \cos \theta + \rho_m E \cos \gamma \cos^2(\psi/2)}{\sigma} \right] + T_m^4 \cos^2\left(\frac{\psi}{2}\right) + \frac{U}{\epsilon \sigma} \right\}^{1/4} \quad (11)$$

The temperature distribution over the surface of an unshielded vehicle at any time during the lunar day can be determined from this equation. The variables that determine the temperature distribution for any specific vehicle with no internally generated heat are simply the sun's illumination angle and the ratio of solar absorptance to emittance, α_s/ϵ , of the vehicle's skin. When internally generated heat is present, the heat flux into the skin and the actual value of emittance of the skin become additional variables.

Thermal conductance.- When a study is made of the effect of skin conductance upon the temperature variation of the vehicle's surface, certain new parameters must be introduced. The conductivity, thickness, and emittance of the surface material, as well as the vehicle's size, now become pertinent parameters. Such an analysis is developed in appendix A and is based upon the relaxation method. This analysis has been developed for one-dimensional heat conduction and may be applied only to sections of a vehicle where the temperature gradients in all other directions are negligible.

Temperatures of Shielded Vehicles

In order to describe adequately the radiative heat-transfer system that consists of a vehicle, solar and lunar radiation shields, the lunar surface, and

space, a more general radiation analysis is required. Such an analysis is developed in appendix B and is summarized here.

The calculation of temperatures resulting from radiative heat transfer between the components of the system is complex because multiple reflections from each surface must be considered. Methods have been developed (e.g., refs. 12, 13, and 14) whereby infinite reflections may be included in a systematic manner, and, with the use of a high-speed computer, the lengthy computations involved in these methods can be readily accomplished.

The method of analysis developed within the present report is similar to that presented in reference 13 but is extended to include radiation absorbed and emitted from both sides of a surface. This analysis includes solar radiation and internally generated heat, as well as emitted radiation. Methods of matrix algebra are used to solve the linear simultaneous equations obtained by a heat balance on specific finite surfaces.

A heat balance can be made on an arbitrary surface i that may receive and emit radiation from both sides (a and b). The heat balance includes direct solar radiation S_i , reflected solar radiation from all surfaces in the system $\sum_{\beta=1}^{\infty} \beta^v_i$, emitted radiation (both direct and reflected) from all surfaces $\sum_{\beta=0}^{\infty} \beta^w_i$, and internal heat U_i . Thus, as in equation (10),

$$\left(\begin{array}{c} \text{direct solar rad-} \\ \text{iation absorbed} \end{array} \right) + \left(\begin{array}{c} \text{reflected solar} \\ \text{radiation absorbed} \end{array} \right) + \left(\begin{array}{c} \text{emitted radiation} \\ \text{absorbed (direct} \\ \text{and reflected)} \end{array} \right) + \left(\begin{array}{c} \text{internal} \\ \text{heat} \end{array} \right) = \left(\begin{array}{c} \text{radiation} \\ \text{emitted} \end{array} \right) \quad (12)$$

or

$$S_i(a) + S_i(b) + \sum_{\beta=1}^{\infty} \beta^v_i(a) + \sum_{\beta=1}^{\infty} \beta^v_i(b) + \sum_{\beta=0}^{\infty} \beta^w_i(a) + \sum_{\beta=0}^{\infty} \beta^w_i(b) + U_i = q_i(a) + q_i(b) \quad (13)$$

where $q_i(a)$ and $q_i(b)$ are the radiation components emitted from sides a and b, respectively. Equation (13) is a set of simultaneous equations from which surface temperatures may be obtained by solving for q_i . Through methods of matrix algebra (details are found in appendix B), the equations may be organized and solved.

RESULTS AND DISCUSSION

The preceding analyses have been developed for evaluating the thermal control of a vehicle on the lunar surface. The basic vehicle configuration

chosen for study is shown in figure 3. It consists of a 60° conical section atop a cylindrical section. The solar and lunar shield configurations added to this basic configuration are shown in figure 4.

The effects of thermal parameters, such as the α_s/ϵ ratio, solar-illumination angle, and surface conductance, on the temperatures and temperature distribution of the unshielded and shielded vehicle are discussed.

Temperatures on an Unshielded Vehicle During a Lunar Day

Incident radiation.- A vehicle will be subjected to incident solar and lunar radiation in varying amounts during a lunar day, depending on its geometry and position on the moon's surface. Equation (9) gives the components of direct solar radiation, reflected solar radiation, and lunar radiation that are incident upon any element of a vehicle. The variation in these components during a lunar day is shown in figure 5 for a strip of elemental width up the conical and cylindrical sections (figs. 5(a) and 5(b), respectively) of the unshielded vehicle being studied. The vehicle is sitting near the lunar equator and the sun moves directly overhead during the lunar day. It can be seen that emitted radiation from the lunar surface is the main component until direct sunlight is incident. The incident solar radiation reaches a maximum when it is normal to the vehicle's surface. As would be expected, the maximum solar radiation is of a much greater magnitude than the maximum lunar radiation.

Temperature variation for various values of α_s/ϵ .- The variables which determine the temperature distribution over a vehicle with a given geometry and no internally generated heat are the sun's illumination angle and the ratio of solar absorptance to emittance of the vehicle's skin. The radiation incident upon an elemental strip of the vehicle at any time was shown in figure 5. The temperatures arising from this incident radiation are shown in figure 6 for various α_s/ϵ ratios under the assumption that no heat is transferred between elements on the vehicle.

The temperatures reached on the vehicle are a strong function of α_s/ϵ during lunar daytime, but during lunar night, the surface properties are immaterial and the vehicle will have an equilibrium temperature that will depend only upon the vehicle geometry and will be between the temperature of the lunar surface (-240° F) and the temperature of space (-460° F).

The maximum temperature is reached at any point on the vehicle when the total absorbed radiation is a maximum. This occurs near the angle for maximum incident solar radiation for surfaces with a high α_s/ϵ ratio, but for surfaces with a low α_s/ϵ ratio, it occurs near the subsolar point. For various realistic surface materials, the maximum temperatures reached on the sections of the vehicle studied are shown in table I.

The curve for $\alpha_s/\epsilon = 0$ in figure 6 is a theoretical limit, representative of the temperature variation during a lunar day on a vehicle that absorbs no solar radiation. This limit may be nearly realized by shielding a vehicle from solar radiation as will be described later.

Temperature of a vehicle at the subsolar point.- A vehicle at the subsolar point is exposed to the maximum radiation emitted from the lunar surface as well as to solar radiation from directly overhead.

The temperatures of the conical and cylindrical sections of the vehicle at the subsolar point are presented in figure 7 as a function of α_s/ϵ ratio. Solar and lunar illumination are uniform over each section so that each section will have a single, uniform temperature. Since the cylindrical section of the vehicle does not receive direct solar radiation and since incident reflected solar radiation is low (see fig. 5(b)), the temperature of the section is relatively insensitive to changes in α_s/ϵ . The temperature of the conical section, however, is strongly dependent upon α_s/ϵ since more than half of the total radiation incident upon the conical section is solar radiation. As the α_s/ϵ ratio of each section approaches zero, the temperatures will approach lower limits that are a function of only the vehicle geometry. The temperatures on the vehicle at this lower limit are 129° F and 35° F (from eq. (11)) for the cylindrical and conical sections, respectively.

Temperature variation around a vehicle illuminated from the side.- A severe thermal problem may occur when an unshielded vehicle is illuminated directly from the side. Side illumination would be encountered at lunar dawn or dusk or if the vehicle were situated near the poles. One side of the vehicle would receive the full intensity of the direct sun, while the other side would be in darkness, "seeing" only a cold, shadowed lunar surface and space.

When there is no conduction in the skin, the temperature distribution around the cylindrical section of the vehicle is as shown in figure 8. The temperature of a vertical strip on the surface of the cylindrical section is plotted against its location angle around the vehicle for various values of α_s/ϵ . It is apparent that large differences in temperature may occur between the sunlit and dark sides of a vehicle, especially at the higher values of α_s/ϵ . Also apparent are the large thermal gradients which are present in the region from about 80° to 90°.

The effect of surface conductance on the temperature distribution around the cylindrical section of the vehicle is determined by the methods presented in appendix A and is shown in figure 9. The vehicle in this example is 10 feet in diameter and its surface has an α_s/ϵ ratio of 1.0. Thermal conductance C in the skin ranges from zero to a value representative of 1/8-inch-thick aluminum. Two cases are presented:

- (a) The emittance of the surface = 0.9 (fig. 9(a))
- (b) The emittance of the surface = 0.1 (fig. 9(b))

It can be seen that, in general, conduction in a vehicle's skin can reduce both the temperature differences and gradients around the vehicle. This is accomplished primarily by raising the dark-side temperature of the vehicle. It can be seen that the use of a surface of low emittance results in lower temperature differences and reduced gradients when compared with one of higher emittance. It is apparent, however, that even for a skin of relatively high conductance (1/8-in. aluminum), a large temperature variation may still exist from one side of the vehicle to the other.

The Use of Solar and Lunar Radiation Shields for Thermal Control of a Vehicle During Lunar Daytime

It has been shown that surface temperatures of an unshielded vehicle may be undesirably high during lunar daytime. Surfaces of very low α_s/ϵ will reduce the amount of solar radiation that is absorbed, as shown earlier, but the hot lunar surface may still provide enough radiation to maintain undesirably high vehicle temperatures. Therefore, shields are now considered as a method of minimizing this problem by reducing both incident solar and incident lunar radiation.

Effectiveness of shielding at the subsolar point.- The shielded vehicle configurations studied are presented in figures 4(a), (b), and (c). A circular shield with the same diameter as the vehicle or larger (figs. 4(a) and 4(b)) was used to eliminate all direct solar radiation on the vehicle. Reflected solar radiation and lunar radiation also may be reduced by means of a shield that is symmetric around the base of the vehicle and is completely shaded by the large solar radiation shield, as shown in figure 4(c).

Temperatures of the conical and cylindrical sections of the unshielded and the three shielded vehicle configurations at the subsolar point were calculated by the methods developed in appendix B, and thus include infinite reflections and reradiations among all surfaces. Results of typical analyses are presented in figure 10 as a function of the α_s/ϵ ratio on the conical and cylindrical sections of the vehicle (figs. 10(a) and 10(b), respectively). The solar shield has a white coating on the sunlit side ($\alpha_s = 0.2$, $\epsilon = 0.8$) and a black coating on the shaded side ($\alpha_s = 1.0$, $\epsilon = 1.0$) and is separated from the apex of the conical section by a distance equal to one vehicle diameter. The lunar radiation shield has a polished metal surface of low emittance ($\alpha_s = 0.2$, $\epsilon = 0.04$).

When a solar shield of the same diameter as the vehicle is added to the unshielded vehicle, the amount of solar radiation incident upon the conical section is greatly reduced (see fig. 10(a)). The surface temperature then becomes relatively independent of the α_s/ϵ ratio and almost equivalent to the temperature of a surface with a theoretical value of $\alpha_s/\epsilon = 0$ (see fig. 6(a)). The reduction in temperature is 36°F for $\alpha_s/\epsilon = 0.2$, 150°F for $\alpha_s/\epsilon = 1.0$, and 378°F for a vehicle whose α_s/ϵ ratio is 5.0. The temperature of the cylindrical section remains relatively unchanged (fig. 10(b)) since the addition of the small shield does not affect the thermal environment of this section to an appreciable degree.

If the size of the shield is increased, the lunar surface around the vehicle will be shaded and thus cooled. As a result, the temperature of the cylindrical section will be reduced. However, the conical section will be hotter because the larger shield restricts radiation from the conical section to space to a greater degree and reradiates more heat from the lunar surface onto the conical section.

Vehicle temperatures may be reduced further by the addition of a lunar radiation shield of the type shown in figure 4(c). With this "skirt shield" of low emittance, the temperatures on the cylindrical section are reduced

considerably and become effectively independent of the α_s/ϵ ratio of the vehicle (fig. 10(b)). Results of additional vehicle-shield studies under various conditions are presented in table II.

It should be remembered that the previous studies were for a vehicle with no internally generated heat. The surface temperatures of a vehicle with internal heat can be calculated by equation (11) for unshielded vehicles and by methods presented in appendix B for shielded vehicles. The internally generated heat, radiating area, and surface emittance now become additional parameters. Through the use of shielding, the external radiation absorbed by the vehicle can be reduced enough to allow a high rate of heat dissipation at a reasonable temperature level. As an example, figure 11 shows that a vehicle with a surface emittance of 1.0 and the dimensions given can dissipate nearly 10 kilowatts of internally generated heat at the subsolar point and still maintain a surface temperature below 100° F. Additional examples for vehicles with various surface properties are listed in table III.

Effectiveness of shielding for side illumination.- Solar and lunar radiation shields can be used at any time during the lunar day, and their design may be optimized for specific mission requirements and allowable temperature ranges. A solar shield may be particularly useful when the vehicle is subjected to side illumination (fig. 4(d)). For this case, there is no need for lunar radiation shields since the emitted lunar radiation is low. As the solar-radiation shield is positioned farther from the vehicle, the temperatures approach values nearly as low as those during lunar night, as shown in figure 12. Thus, by means of shielding, the large temperature variation noted for the unshielded vehicle (see figs. 8 and 9) may be eliminated.

In summary, shields are most effective when they isolate a vehicle from external radiation and at the same time do not appreciably restrict the emission of radiation from the vehicle to space. Since shields can eliminate nearly all of the solar radiation that is incident upon a vehicle, the temperature of the vehicle, in effect, becomes almost independent of its α_s/ϵ ratio. Thus, acceptably low surface temperatures could be achieved without the problems associated with obtaining very low α_s/ϵ surfaces. Moreover, possible changes in the solar absorptance characteristics of a surface due to environmental exposure would not cause undesirable changes in surface temperature.

CONCLUDING REMARKS

The analyses presented herein have indicated that radiation shields can be used as an effective method of thermal control for vehicles on the lunar surface. The shields can effectively isolate the vehicle from both solar and lunar radiation during daytime.

For purposes of comparison, a basic vehicle configuration was chosen for study, although the analyses are applicable to any vehicle within the limits of the assumptions. A study of the surface temperatures of the unshielded vehicle showed that very low α_s/ϵ surfaces are needed to maintain low temperatures during the lunar day. However, even with these surfaces, at or near the subsolar

point, the vehicle's temperature may be undesirably high as a result of lunar radiation that is absorbed by the vehicle. Unshielded vehicles that are illuminated from the side (at lunar dawn, dusk, or at poles) will have a large temperature difference, and will have high temperature gradients, from their sunlit to their shaded side, even when their skin conductance is fairly high.

Solar-radiation shields may be used to isolate a lunar vehicle from direct solar radiation. The temperature of the vehicle becomes independent of the α_s/ϵ ratio of its surface if shielded from all solar radiation, and is dependent only upon how much radiation is incident from the lunar surface and/or shields. The radiation from the lunar surface may be greatly reduced by lunar-radiation shields. When both forms of shielding are used, a vehicle with no unusual or extreme surface properties can be adequately thermally protected during lunar daytime.

A vehicle designed for operation during lunar night probably requires a surface with low emittance and may experience severe thermal problems if, because of some unforeseen circumstance, it is forced to operate during lunar daytime. (A surface of low emittance will probably have a high α_s/ϵ ratio and, consequently, high temperatures during lunar daytime.) The thermal protection of solar and lunar radiation shielding can be as effective for this type of vehicle as for those designed for operation during lunar daytime.

Ames Research Center

National Aeronautics and Space Administration
Moffett Field, Calif., Oct. 3, 1963

APPENDIX A

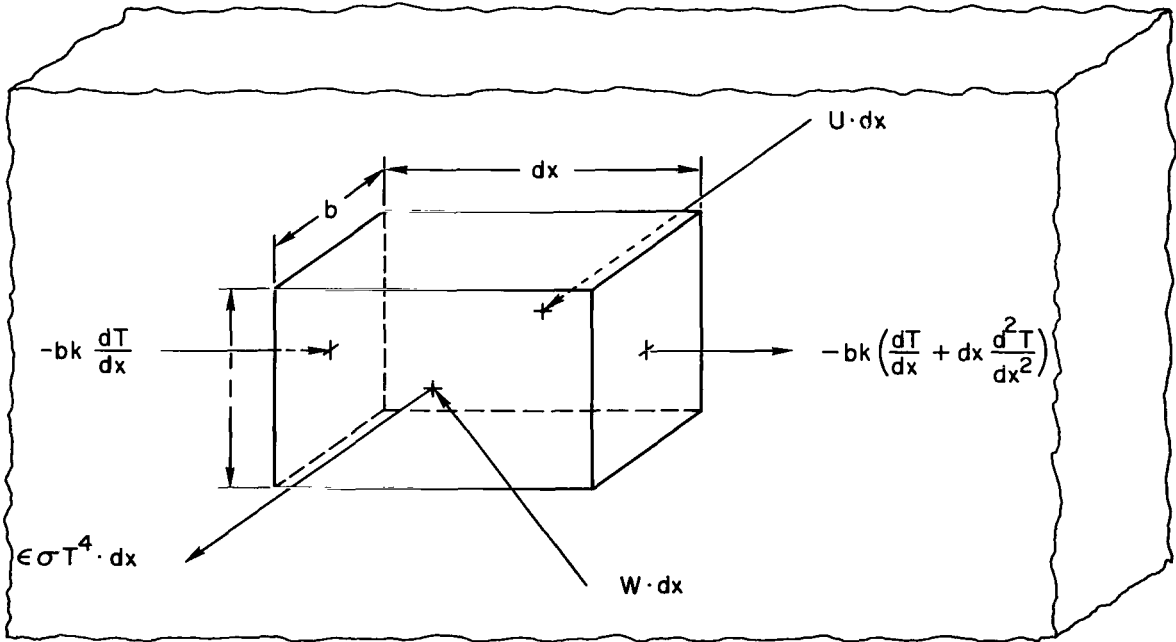
ANALYSIS OF ONE-DIMENSIONAL CONDUCTANCE IN A RADIATING SURFACE

The assumption of zero conductance in the surface of a vehicle may cause an appreciable error in the temperature distribution over the surface of vehicles illuminated from the side when the conductance in the skin is large. A one-dimensional analysis is developed to evaluate the effect of conductance upon the temperature distribution around sections of vehicles where the temperature gradients are negligible in all but one direction.

An equilibrium heat balance on an elemental volume of the vehicle's skin (see sketch (a)) is made by equating the sum of the total external radiation absorbed per unit area W , the internal heat per unit area from within the vehicle U , and the net heat conducted into the element Q_c to the radiation flux emitted from the element $\epsilon\sigma T^4$.

Thus,

$$(W + U)dx + Q_c = \epsilon\sigma T^4 dx \quad (A1)$$



Sketch (a)

where

$$Q_c = bk \frac{d^2T}{dx^2} dx \quad (A2)$$

and b is the skin thickness and k is the conductivity. Thus,

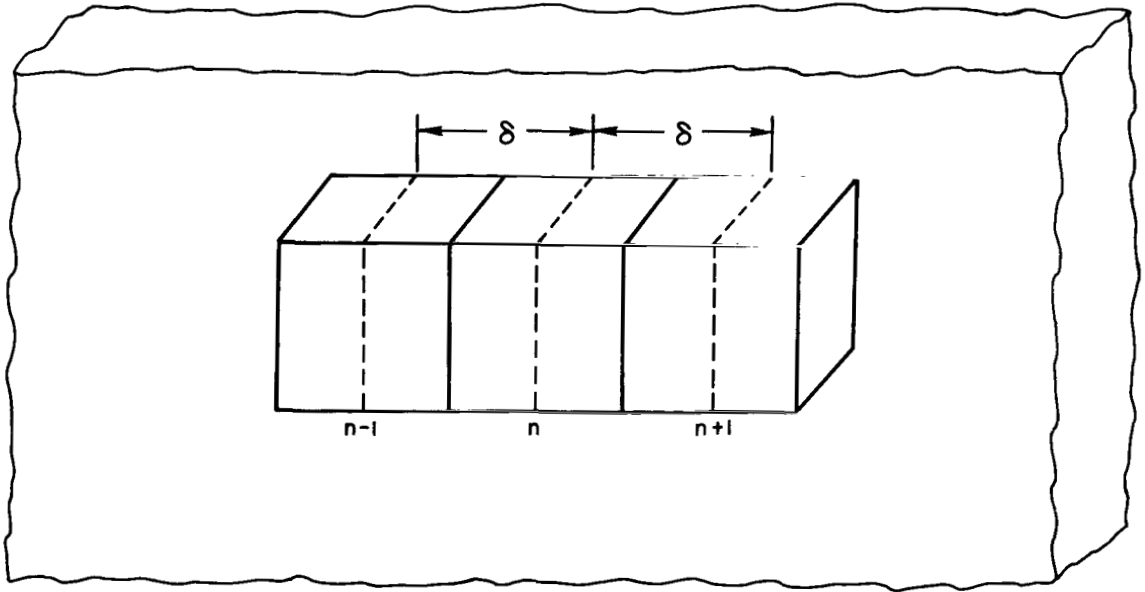
$$(W + U) + bk \frac{d^2 T}{dx^2} = \epsilon \sigma T^4 \quad (A3)$$

or

$$\frac{d^2 T}{dx^2} = \frac{\epsilon \sigma}{bk} T^4 - \frac{(W + U)}{bk} \quad (A4)$$

This resulting equation is nonlinear and numerical methods are needed to solve it for a particular case. A technique particularly applicable to the solution of equation (A4) is the relaxation method (see ref. 15). Equation (A4) may be written in a finite-difference form relating the temperatures of the adjacent elements to the temperature and heat balance of the n th element (see sketch (b)):

$$T_{n-1} + T_{n+1} - 2T_n = \left[\frac{\epsilon \sigma}{bk} T_n^4 - \frac{(W + U)}{bk} \right] \delta^2 \quad (A5)$$



Sketch (b)

$$T_{n-1} + T_{n+1} - \left(2T_n + \frac{\epsilon}{bk} \delta^2 T_n^4 \right) + \frac{(W + U)}{bk} \delta^2 = R_n \quad (A6)$$

The residual of the n th element, R_n , is reduced to zero when the correct elemental temperatures are computed. Equation (A6), with suitable boundary

conditions, will yield the temperature distribution around the vehicle when the external and internal heat inputs, skin thickness and conductivity, and the conduction length δ necessary for the desired accuracy are given.

APPENDIX B

A GENERAL ANALYSIS OF RADIATION INTERCHANGE AMONG SURFACES

Consider n finite, isothermal surfaces that are oriented in space in an arbitrary manner. The surfaces are of arbitrary shape and emit and reflect diffusely. The two sides of a typical surface will be designated as a and b , respectively. The direct solar radiation absorbed by the a side of the i th surface can be expressed as

$$S_i(a) = a_i \alpha_{si}(a) I_i(a) \quad (B1)$$

where

a_i area of i th surface

$\alpha_{si}(a)$ absorptance of the a side of the i th surface

$I_i(a)$ solar radiation flux incident upon the a side of the i th surface

Reflected solar radiation from the i th surface may be expressed as

$$r_i(a) = a_i [1 - \alpha_{si}(a)] I_i(a) \quad (B2)$$

The thermal radiation from the same surface is given by

$$q_i(a) = a_i \epsilon_i(a) \sigma T_i^4 \quad (B3)$$

where

σ Boltzmann's constant

$\epsilon_i(a)$ emittance of the a side of the i th surface

T_i absolute temperature of the i th surface

Additional radiation inputs to each surface come from the summation of all the reflections that occur among all the sides of all the surfaces. For example, solar radiation absorbed by the a side of the i th surface, for the case of a single reflection from all surfaces, is expressed by the following summation:

$$i^v_i(a) = \left[\sum_{j=1}^n r_j(a) f_{ji}(a) + \sum_{j=1}^n r_j(b) f_{ji}(a) \right] \alpha_{si}(a) \quad (B4)$$

where the prescript 1 denotes number of reflections and

$f_j(b)i(a)$ radiation configuration factor from the b side of the ith surface to the a side of the ith surface

The solar radiation absorbed by the b side of the ith surface after one reflection is given by

$$1V_i(b) = \left[\sum_{j=1}^n r_j(a) f_j(a)i(b) + \sum_{j=1}^n r_j(b) f_j(b)i(b) \right] \alpha_{s_i(b)} \quad (B5)$$

The writing of these equations can be simplified through the use of a summation convention: Whenever an index occurs two or more times in a term on the right side of the equation but not on the left side, that term is to be summed over the given index. Using this convention, we write equations (B4) and (B5) as

$$1V_i(a) = \left[r_j(a) f_j(a)i(a) + r_j(b) f_j(b)i(a) \right] \alpha_{s_i(a)} \quad (B6)$$

$$1V_i(b) = \left[r_j(a) f_j(a)i(b) + r_j(b) f_j(b)i(b) \right] \alpha_{s_i(b)} \quad (B7)$$

For energy absorbed after two reflections (prescript is 2), there is a summation for the first reflection to all sides; then there is a summation of the resulting reflections from all sides to the given surface. Thus, for the a side of the ith surface, the total summation may be expressed as

$$\begin{aligned} 2V_i(a) = & \left\{ \sum_{k=1}^n \left[\sum_{j=1}^n r_j(a) f_j(a)k(a) + \sum_{j=1}^n r_j(b) f_j(b)k(a) \right] \left[1 - \alpha_{s_k(a)} \right] f_{k(a)i(a)} \right. \\ & \left. + \sum_{k=1}^n \left[\sum_{j=1}^n r_j(a) f_j(a)k(b) + \sum_{j=1}^n r_j(b) f_j(b)k(b) \right] \left[1 - \alpha_{s_k(b)} \right] f_{k(b)i(a)} \right\} \alpha_{s_i(a)} \end{aligned} \quad (B8)$$

Upon rearrangement and use of the summation convention, equation (B8) can be put in the form

$$\begin{aligned} 2V_i(a) = & \left(r_j(a) \left\{ f_j(a)k(a) \left[1 - \alpha_{s_k(a)} \right] f_{k(a)i(a)} \right. \right. \\ & + \left. f_j(a)k(b) \left[1 - \alpha_{s_k(b)} \right] f_{k(b)i(a)} \right\} + r_j(b) \left\{ f_j(b)k(a) \left[1 - \alpha_{s_k(a)} \right] f_{k(a)i(a)} \right. \\ & \left. \left. + f_j(b)k(b) \left[1 - \alpha_{s_k(b)} \right] f_{k(b)i(a)} \right\} \right) \alpha_{s_i(a)} \end{aligned} \quad (B9)$$

In a similar manner the energy absorbed by the b side of the ith surface after two reflections is found to be

$$\begin{aligned}
 2v_i(b) = & \left(r_j(a) \left\{ f_j(a)k(a) \left[1 - \alpha_{sk(a)} \right] f_k(a)i(b) \right. \right. \\
 & + f_j(a)k(b) \left[1 - \alpha_{sk(b)} \right] f_k(b)i(b) \left. \right\} + r_j(b) \left\{ f_j(b)k(a) \left[1 - \alpha_{sk(a)} \right] f_k(a)i(b) \right. \\
 & \left. \left. + f_j(b)k(b) \left[1 - \alpha_{sk(b)} \right] f_k(b)i(b) \right\} \right) \alpha_{si(b)} \quad (B10)
 \end{aligned}$$

Subsequent terms for more reflections become more elaborate but follow a similar pattern of construction as one additional example will show:

$$\begin{aligned}
 3v_i(a) = & \left[r_j(a) \left(f_j(a)k(a) \left[1 - \alpha_{sk(a)} \right] \left\{ f_k(a)l(a) \left[1 - \alpha_{sl(a)} \right] f_l(a)i(a) \right. \right. \right. \\
 & + f_k(a)l(b) \left[1 - \alpha_{sl(b)} \right] f_l(b)i(a) \left. \right\} \\
 & + f_j(a)k(b) \left[1 - \alpha_{sk(b)} \right] \left\{ f_k(b)l(a) \left[1 - \alpha_{sl(a)} \right] f_l(a)i(a) \right. \\
 & \left. \left. + f_k(b)l(b) \left[1 - \alpha_{sl(b)} \right] f_l(b)i(a) \right\} \right) \\
 & + r_j(b) \left(f_j(b)k(a) \left[1 - \alpha_{sk(a)} \right] \left\{ f_k(a)l(a) \left[1 - \alpha_{sl(a)} \right] f_l(a)i(a) \right. \right. \\
 & + f_k(a)l(b) \left[1 - \alpha_{sl(b)} \right] f_l(b)i(a) \left. \right\} \\
 & + f_j(b)k(b) \left[1 - \alpha_{sk(b)} \right] \left\{ f_k(b)l(a) \left[1 - \alpha_{sl(a)} \right] f_l(a)i(a) \right. \\
 & \left. \left. + f_k(b)l(b) \left[1 - \alpha_{sl(b)} \right] f_l(b)i(a) \right\} \right) \right] \alpha_{si(a)} \quad (B11)
 \end{aligned}$$

The equations for the inputs due to multiple reflections of the emitted radiation from all sides of all surfaces have the same form as the preceding equations. These equations can be obtained by replacing r, v, and α_s by the corresponding terms for emitted radiation q, w, and ϵ , respectively (q has been previously defined by equation (B3)). Thus, $o^w_i(a)$ has the form

$$o^w_i(a) = \left[q_j(a) f_j(a)i(a) + q_j(b) f_j(b)i(a) \right] \epsilon_i(a) \quad (B12)$$

A heat balance may now be made upon the surface including internally generated heat:

$$\begin{aligned} \text{Heat emitted} = & \left(\begin{array}{c} \text{solar radiation absorbed} \\ \text{(direct and reflected)} \end{array} \right) + \left(\begin{array}{c} \text{emitted radiation absorbed} \\ \text{(direct and reflected)} \end{array} \right) \\ & + (\text{internal heat}) \end{aligned} \quad (\text{B13})$$

Internal heat may be treated as an external input and treated in exactly the same way as the absorbed direct solar radiation.

$$q_i(a) + q_i(b) = S_i(a) + S_i(b) + U_i a_i + \sum_{\beta=1}^{\infty} \beta^V i(a) + \sum_{\beta=1}^{\infty} \beta^V i(b) + \sum_{\beta=0}^{\infty} \beta^W i(a) + \sum_{\beta=0}^{\infty} \beta^W i(b) \quad (\text{B14})$$

where the prescript β denotes number of reflections. Equation (B14) is a set of simultaneous equations which contain sums within sums, etc. The methods of matrix algebra are particularly valuable in organizing and solving such expressions. As a first step, the following matrices are defined:

$$\left. \begin{aligned} \bar{A}_a &\equiv \begin{bmatrix} \alpha_{s1}(a) & 0 & \dots & 0 \\ 0 & \alpha_{s2}(a) & & 0 \\ \cdot & \cdot & \cdot & \cdot \\ \cdot & \cdot & \cdot & \cdot \\ 0 & 0 & & \alpha_{sn}(a) \end{bmatrix} & \bar{A}_b &\equiv \begin{bmatrix} \alpha_{s1}(b) & 0 & \dots & 0 \\ 0 & \alpha_{s2}(b) & & 0 \\ \cdot & \cdot & \cdot & \cdot \\ \cdot & \cdot & \cdot & \cdot \\ 0 & 0 & \dots & \alpha_{sn}(b) \end{bmatrix} \\ \bar{E}_a &\equiv \begin{bmatrix} \epsilon_1(a) & 0 & \dots & 0 \\ 0 & \epsilon_2(a) & & 0 \\ \cdot & \cdot & \cdot & \cdot \\ \cdot & \cdot & \cdot & \cdot \\ 0 & 0 & \dots & \epsilon_n(a) \end{bmatrix} & \bar{E}_b &\equiv \begin{bmatrix} \epsilon_1(b) & 0 & \dots & 0 \\ 0 & \epsilon_2(b) & & 0 \\ \cdot & \cdot & \cdot & \cdot \\ \cdot & \cdot & \cdot & \cdot \\ 0 & 0 & & \epsilon_n(b) \end{bmatrix} \\ \bar{F}_{ab} &\equiv \begin{bmatrix} f_{1(a)1(b)} & f_{1(a)2(b)} & \dots & f_{1(a)n(b)} \\ f_{2(a)1(b)} & f_{2(a)2(b)} & \dots & f_{2(a)n(b)} \\ \cdot & \cdot & \cdot & \cdot \\ \cdot & \cdot & \cdot & \cdot \\ f_{n(a)1(b)} & f_{n(a)2(b)} & \dots & f_{n(a)n(b)} \end{bmatrix} & & \text{with similar} \\ & & & & \text{expressions for} \\ & & & & \bar{F}_{ba}, \bar{F}_{aa}, \text{ and } \bar{F}_{bb} \\ \bar{S}_a &\equiv \begin{bmatrix} S_1(a) & S_2(a) & \dots & S_n(a) \end{bmatrix} & \bar{S}_b &\equiv \begin{bmatrix} S_1(b) & S_2(b) & \dots & S_n(b) \end{bmatrix} \\ \bar{R}_a &\equiv \begin{bmatrix} r_1(a) & r_2(a) & \dots & r_n(a) \end{bmatrix} & \bar{R}_b &\equiv \begin{bmatrix} r_1(b) & r_2(b) & \dots & r_n(b) \end{bmatrix} \\ \bar{U} &\equiv \begin{bmatrix} U_1 a_1 & U_2 a_2 & \dots & U_n a_n \end{bmatrix} & \bar{Q} &\equiv \begin{bmatrix} a_1 T_1^4 & a_2 T_2^4 & \dots & a_n T_n^4 \end{bmatrix} \end{aligned} \right\} \quad (\text{B15})$$

With these definitions, we may now write the radiation heat-transfer expressions in matrix form. For example the array of terms,

$$f_{j(a)k(b)} \left[1 - \alpha_{sk(b)} \right] \equiv \bar{F}_{ab}(\bar{I} - \bar{A}_b) \quad j, k = 1, 2 \dots n \quad (B16)$$

where

$$\bar{I} = \begin{bmatrix} 1 & 0 & \dots & 0 \\ 0 & 1 & \dots & 0 \\ \cdot & \cdot & & \cdot \\ \cdot & \cdot & & \cdot \\ \cdot & \cdot & & \cdot \\ 0 & 0 & & 1 \end{bmatrix} \quad (B17)$$

is a unit matrix. Equation (B14) may now be written in matrix form as

$$\begin{aligned} \bar{Q}(\bar{E}_a + \bar{E}_b) &= \bar{S}_a + \bar{S}_b + \bar{U} + \bar{R}_a \left[\bar{H}_{aa} \bar{A}_a + \bar{H}_{ab} \bar{A}_b \right] + \bar{R}_b \left[\bar{H}_{ba} \bar{A}_a + \bar{H}_{bb} \bar{A}_b \right] \\ &+ \bar{Q} \bar{E}_a \left[\bar{G}_{aa} \bar{E}_a + \bar{G}_{ab} \bar{E}_b \right] + \bar{Q} \bar{E}_b \left[\bar{G}_{ba} \bar{E}_a + \bar{G}_{bb} \bar{E}_b \right] \end{aligned} \quad (B18)$$

The \bar{H} and \bar{G} matrices may be termed "radiation transfer matrices" and are given by

$$\left. \begin{aligned} \bar{H}_{aa} &= \bar{F}_{aa} + \bar{F}_{aa}(\bar{I} - \bar{A}_a)\bar{F}_{aa} + \bar{F}_{ab}(\bar{I} - \bar{A}_b)\bar{F}_{ba} + \bar{F}_{aa}(\bar{I} - \bar{A}_a) \left[\bar{F}_{aa}(\bar{I} - \bar{A}_a)\bar{F}_{aa} + \bar{F}_{ab}(\bar{I} - \bar{A}_b)\bar{F}_{ba} \right] \\ &+ \bar{F}_{ab}(\bar{I} - \bar{A}_b) \left[\bar{F}_{ba}(\bar{I} - \bar{A}_a)\bar{F}_{aa} + \bar{F}_{bb}(\bar{I} - \bar{A}_b)\bar{F}_{ba} \right] + \dots \\ \bar{H}_{ab} &= \bar{F}_{ab} + \bar{F}_{aa}(\bar{I} - \bar{A}_a)\bar{F}_{ab} + \bar{F}_{ab}(\bar{I} - \bar{A}_b)\bar{F}_{bb} + \bar{F}_{aa}(\bar{I} - \bar{A}_a) \left[\bar{F}_{aa}(\bar{I} - \bar{A}_a)\bar{F}_{ab} + \bar{F}_{ab}(\bar{I} - \bar{A}_b)\bar{F}_{bb} \right] \\ &+ \bar{F}_{ab}(\bar{I} - \bar{A}_b) \left[\bar{F}_{ba}(\bar{I} - \bar{A}_a)\bar{F}_{ab} + \bar{F}_{bb}(\bar{I} - \bar{A}_b)\bar{F}_{bb} \right] + \dots \\ \bar{H}_{ba} &= \bar{F}_{ba} + \bar{F}_{ba}(\bar{I} - \bar{A}_a)\bar{F}_{aa} + \bar{F}_{bb}(\bar{I} - \bar{A}_b)\bar{F}_{ba} + \bar{F}_{ba}(\bar{I} - \bar{A}_a) \left[\bar{F}_{aa}(\bar{I} - \bar{A}_a)\bar{F}_{aa} + \bar{F}_{ab}(\bar{I} - \bar{A}_b)\bar{F}_{ba} \right] \\ &+ \bar{F}_{bb}(\bar{I} - \bar{A}_b) \left[\bar{F}_{ba}(\bar{I} - \bar{A}_a)\bar{F}_{ab} + \bar{F}_{bb}(\bar{I} - \bar{A}_b)\bar{F}_{bb} \right] + \dots \\ \bar{H}_{bb} &= \bar{F}_{bb} + \bar{F}_{ba}(\bar{I} - \bar{A}_a)\bar{F}_{ab} + \bar{F}_{bb}(\bar{I} - \bar{A}_b)\bar{F}_{bb} + \bar{F}_{ba}(\bar{I} - \bar{A}_a) \left[\bar{F}_{aa}(\bar{I} - \bar{A}_a)\bar{F}_{ab} + \bar{F}_{ab}(\bar{I} - \bar{A}_b)\bar{F}_{bb} \right] \\ &+ \bar{F}_{bb}(\bar{I} - \bar{A}_b) \left[\bar{F}_{ba}(\bar{I} - \bar{A}_a)\bar{F}_{ab} + \bar{F}_{bb}(\bar{I} - \bar{A}_b)\bar{F}_{bb} \right] + \dots \end{aligned} \right\} \quad (B19)$$

The \bar{A} matrices are replaced by the corresponding \bar{E} matrices to obtain the \bar{G} matrices.

The patterns of the subscripts a and b suggest that an additional concept of matrix algebra may be utilized, namely, that matrices themselves may be used as elements of matrices. Thus, for example,

$$\bar{A} = \begin{bmatrix} \bar{A}_a & \bar{O} \\ \bar{O} & \bar{A}_b \end{bmatrix}, \quad \bar{E} = \begin{bmatrix} \bar{E}_a & \bar{O} \\ \bar{O} & \bar{E}_b \end{bmatrix}, \quad \bar{F} = \begin{bmatrix} \bar{F}_{aa} & \bar{F}_{ab} \\ \bar{F}_{ba} & \bar{F}_{bb} \end{bmatrix} \quad (B20)$$

where \bar{O} is the null or zero matrix. With this concept, the following expression for \bar{H}_{aa} , for example, may be verified:

$$\begin{aligned} \bar{H}_{aa} = & \bar{F}_{aa} + \left[\bar{F}_{aa}(\bar{I} - \bar{A}_a), \bar{F}_{ab}(\bar{I} - \bar{A}_b) \right] \begin{bmatrix} \bar{F}_{aa} \\ \bar{F}_{ba} \end{bmatrix} \\ & + \left[\bar{F}_{aa}(\bar{I} - \bar{A}_a), \bar{F}_{ab}(\bar{I} - \bar{A}_b) \right] \begin{bmatrix} \bar{F}_{aa}(\bar{I} - \bar{A}_a), \bar{F}_{ab}(\bar{I} - \bar{A}_b) \\ \bar{F}_{ba}(\bar{I} - \bar{A}_a), \bar{F}_{bb}(\bar{I} - \bar{A}_b) \end{bmatrix} \begin{bmatrix} \bar{F}_{aa} \\ \bar{F}_{ba} \end{bmatrix} \\ & + \left[\bar{F}_{aa}(\bar{I} - \bar{A}_a), \bar{F}_{ab}(\bar{I} - \bar{A}_b) \right] \begin{bmatrix} \bar{F}_{aa}(\bar{I} - \bar{A}_a), \bar{F}_{ab}(\bar{I} - \bar{A}_b) \\ \bar{F}_{ba}(\bar{I} - \bar{A}_a), \bar{F}_{bb}(\bar{I} - \bar{A}_b) \end{bmatrix}^2 \begin{bmatrix} \bar{F}_{aa} \\ \bar{F}_{ba} \end{bmatrix} + \dots \end{aligned} \quad (B21)$$

which reduces to

$$\bar{H}_{aa} = \bar{F}_{aa} + \left[\bar{F}_{aa}, \bar{F}_{ab} \right] (\bar{I} - \bar{A}) \left\{ \bar{I} + \bar{F}(\bar{I} - \bar{A}) + \left[\bar{F}(\bar{I} - \bar{A}) \right]^2 + \dots \right\} \begin{bmatrix} \bar{F}_{aa} \\ \bar{F}_{ba} \end{bmatrix} \quad (B22)$$

The infinite summation is in the same form as a geometric series. Matrix algebra will allow many results of ordinary algebra to be used, so that the series may be replaced by its sum and equation (B22) becomes

$$\bar{H}_{aa} = \bar{F}_{aa} + \left[\bar{F}_{aa}, \bar{F}_{ab} \right] (\bar{I} - \bar{A}) \left[\bar{I} - \bar{F}(\bar{I} - \bar{A}) \right]^{-1} \begin{bmatrix} \bar{F}_{aa} \\ \bar{F}_{ba} \end{bmatrix} \quad (B23)$$

Similar results may be obtained for the rest of the \bar{H} matrices and for the \bar{G} matrices. When equation (B18) is simplified by combining matrices, it may be written as

$$\begin{aligned} \bar{Q}(\bar{E}_a + \bar{E}_b) = \bar{S}_a + \bar{S}_b + \bar{U} + \begin{bmatrix} \bar{R}_a & \bar{R}_b \end{bmatrix} \begin{bmatrix} \bar{H}_{aa} & \bar{H}_{ab} \\ \bar{H}_{ba} & \bar{H}_{bb} \end{bmatrix} \begin{bmatrix} \bar{A}_a \\ \bar{A}_b \end{bmatrix} \\ + \bar{Q}(\bar{E}_a + \bar{E}_b) \begin{bmatrix} \bar{G}_{aa} & \bar{G}_{ab} \\ \bar{G}_{ba} & \bar{G}_{bb} \end{bmatrix} \begin{bmatrix} \bar{E}_a \\ \bar{E}_b \end{bmatrix} \end{aligned} \quad (B24)$$

This equation may now be solved for \bar{Q} :

$$\bar{Q} = \left(\bar{S}_a + \bar{S}_b + \bar{U} + \begin{bmatrix} \bar{R}_a & \bar{R}_b \end{bmatrix} \bar{H} \begin{bmatrix} \bar{A}_a \\ \bar{A}_b \end{bmatrix} \right) \left(\bar{E}_a + \bar{E}_b - \begin{bmatrix} \bar{E}_a & \bar{E}_b \end{bmatrix} \bar{G} \begin{bmatrix} \bar{E}_a \\ \bar{E}_b \end{bmatrix} \right)^{-1} \quad (B25)$$

where

$$\bar{H} = \begin{bmatrix} \bar{H}_{aa} & \bar{H}_{ab} \\ \bar{H}_{ba} & \bar{H}_{bb} \end{bmatrix} \quad (B26)$$

and

$$\bar{G} = \begin{bmatrix} \bar{G}_{aa} & \bar{G}_{ab} \\ \bar{G}_{ba} & \bar{G}_{bb} \end{bmatrix} \quad (B27)$$

Equation (B25) is the solution to the heat balance on all surfaces. The temperatures of the surfaces can be determined from the definition of \bar{Q} from equations (B15).

REFERENCES

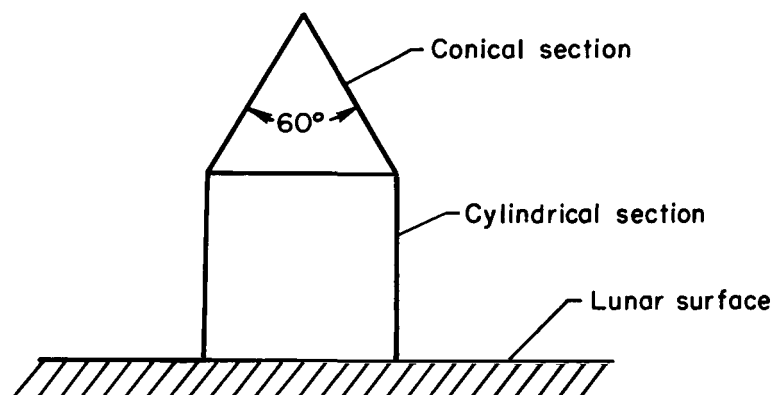
1. Sinton, W. M.: Temperatures on the Lunar Surface. Ch. 11 of Physics and Astronomy of the Moon, Zdenek Kopal, ed., Academic Press, 1962, pp. 407-427.
2. McKellar, L. A.: Effects of the Spacecraft Environment on Thermal Control Materials Characteristics. Proc. Spacecraft Thermodynamics Symposium, San Francisco, 1962, pp. 99-128.
3. Nothwang, George J., Arvesen, John C., and Hamaker, Frank M.: Analysis of Solar-Radiation Shields for Temperature Control of Space Vehicles Subjected to Large Changes in Solar Energy. NASA TN D-1209, 1962.
4. Stevenson, Jack A., and Grafton, John C.: Lunar Temperature Environment. Proc. Inst. Environmental Sci., Los Angeles, 1960, pp. 233-242.
5. Pettit, Edison, and Nicholson, Seth B.: Lunar Radiation and Temperatures. Astrophysical Jour., vol. 71, 1930, pp. 102-135.
6. Sinton, William M.: A Pyrometer for Planetary Temperature Measurements. Lowell Observatory Bulletin no. 104, vol. 4:16, 1959, pp. 260-263.
7. Geoffrion, Ann R., Korner, Marjorie, and Sinton, W. M.: Isothermal Contours of the Moon. Lowell Observatory Bulletin no. 106, vol. 5:1, 1960, pp. 1-15.
8. Pettit, Edison: Radiation Measurements on the Eclipsed Moon. Astrophysical Jour., vol. 91, 1940, pp. 408-420.
9. Jaeger, J. C., and Harper, A. F. A.: Nature of the Surface of the Moon. Nature, London, 166, Dec. 16, 1950, p. 1026.
10. Kopal, Zdenek: Topography of the Moon. Ch. 7 of Physics and Astronomy of the Moon, Zdenek Kopal, ed., Academic Press, 1962, pp. 231-281.
11. Hamilton, D. C., and Morgan, W. R.: Radiant-Interchange Configuration Factors. NACA TN 2836, 1952.
12. Stevenson, J. A., and Grafton, J. C.: Radiation Heat Transfer Analysis for Space Vehicles. Aeronautical Systems Div. TR 61-119, Pt. I, 1961.
13. Petersen, M. W.: Analytical Radiation Phase of High Temperature Research and Development Program ESO 5227. North American Aviation Inc., Rep. NA56-399, 1956.
14. Oppenheim, A. K.: Radiation Analysis by the Network Method. ASME Paper 54-A-75.
15. Schneider, Paul J.: Conduction Heat Transfer. Addison-Wesley Publishing Co., Inc., Cambridge, Mass. 1955.

TABLE I.- MAXIMUM SURFACE TEMPERATURE DURING A LUNAR DAY FOR UNSHIELDED VEHICLE

Type of surface	α_s/ϵ	Maximum temperatures, °F	
		Cylindrical section	Conical section
Tabor solar collector	17.0-7.0	988-701	992-706
Metals	9.0-2.0	776-392	781-403
Silicon solar cells	1.10	289	293
Ideal gray surface	1.0	270	278
White paints	0.5-0.15	189-135	182-82

TABLE II.- EFFECTIVENESS OF SOLAR AND LUNAR RADIATION SHIELDS UPON THE TEMPERATURES OF A VEHICLE AT THE SUBSOLAR POINT; CONDUCTANCE AND INTERNAL HEAT BOTH ZERO

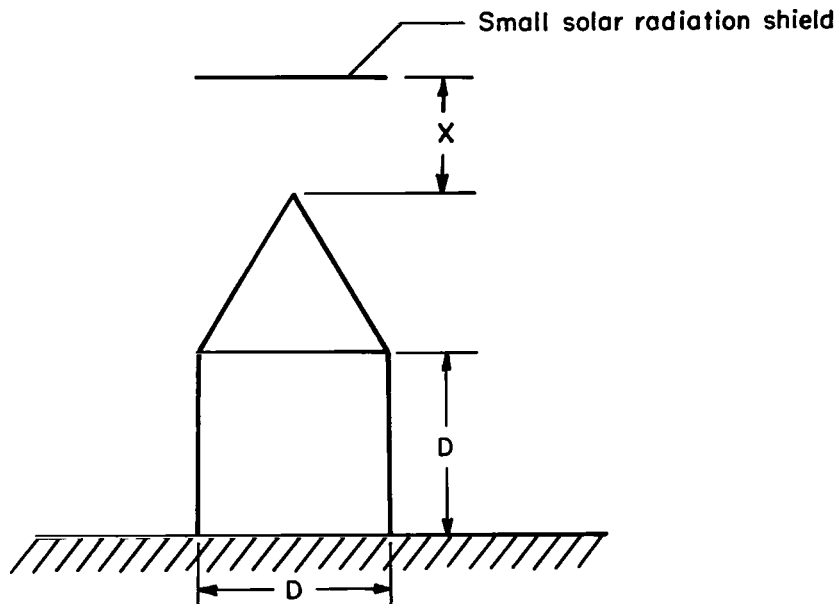
(a) Unshielded vehicle



Vehicle α_s/ϵ	Surface temperature, °F	
	Conical section	Cylindrical section
0.2	83	137
1.0	204	146
5.0	464	184

TABLE II.- EFFECTIVENESS OF SOLAR AND LUNAR RADIATION SHIELDS UPON THE TEMPERATURES OF A VEHICLE AT THE SUBSOLAR POINT; CONDUCTANCE AND INTERNAL HEAT BOTH ZERO - Continued

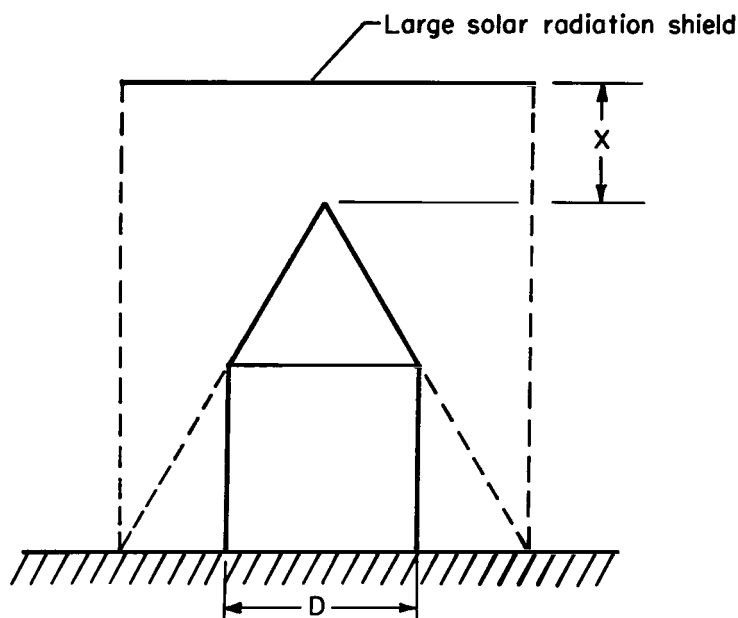
(b) Small solar radiation shield



Surface properties					Separation distance, X/D	Temperatures, °F		
Vehicle	Solar shield					Solar shield	Conical section	Cylindrical section
	Sunlit side		Shaded side					
	α_S/ϵ	α_S	ϵ	α_S				
1.0	1.0	1.0	1.0	1.0	0.25	244	79	146
↓	↓	↓	↓	↓	.50	247	69	146
					.75	249	63	147
					1.00	250	59	147
	.2	.8			.25	169	67	146
	↓	↓			.50	175	61	146
	↓	↓			.75	178	57	146
	↓	↓			1.00	180	54	146
.2	↓	↓	↓	↓	1.00	180	47	135
5.0	↓	↓	↓	↓	1.00	180	86	185

TABLE II.- EFFECTIVENESS OF SOLAR AND LUNAR RADIATION SHIELDS UPON THE TEMPERATURES OF A VEHICLE AT THE SUBSOLAR POINT; CONDUCTANCE AND INTERNAL HEAT BOTH ZERO - Continued

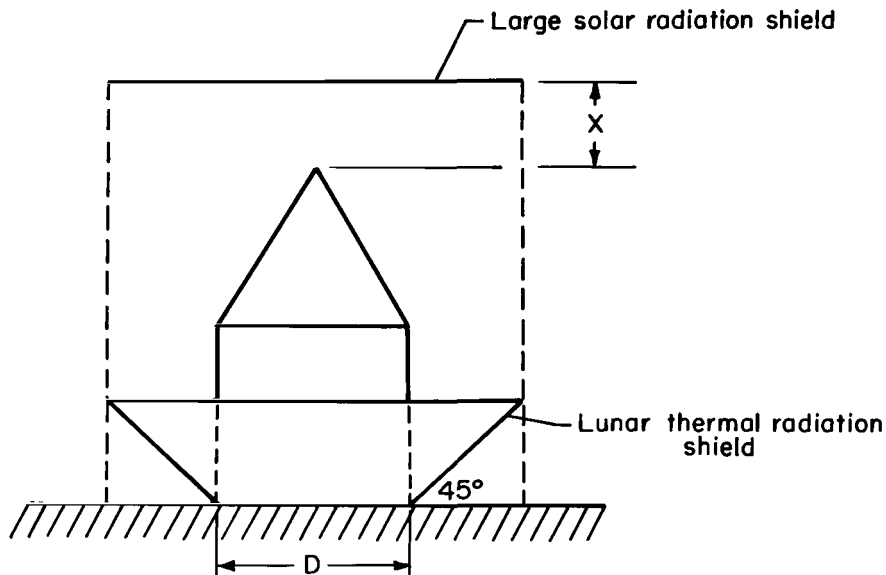
(c) Large solar radiation shield



Surface properties					Separation distance, X/D	Temperatures, °F		
Vehicle	Solar shield					Solar shield	Conical section	Cylindrical section
	Sunlit side		Shaded side					
	α_S/ϵ	α_S	ϵ	α_S				
1.0	1.0	1.0	1.0	1.0	0.25	242	141	93
↓	↓	↓	↓	↓	.50	242	122	92
					.75	242	106	92
					1.00	242	95	92
		.2	.8		.25	165	111	88
		↓	↓		.50	166	96	88
					.75	167	86	88
					1.00	167	78	88
.2	↓	↓	↓	↓	1.00	167	72	80
5.0	↓	↓	↓	↓	1.00	167	106	121

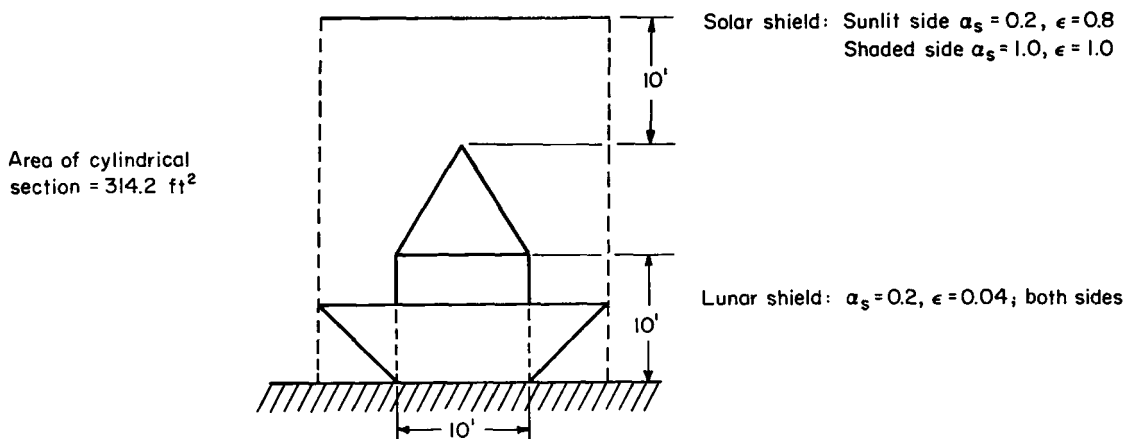
TABLE II. - EFFECTIVENESS OF SOLAR AND LUNAR RADIATION SHIELDS UPON THE TEMPERATURES OF A VEHICLE AT THE SUBSOLAR POINT; CONDUCTANCE AND INTERNAL HEAT BOTH ZERO - Concluded

(d) Solar radiation shield and lunar radiation shield



Surface properties							Separation distance, X/D	Temperatures, °F			
Vehicle	Solar shield				Lunar shield			Solar shield	Lunar shield	Conical section	Cylindrical section
	Sunlit side		Shaded side								
α_s/ϵ	α_s	ϵ	α_s	ϵ	α_s	ϵ					
1.0	1.0	1.0	1.0	1.0	1.0	1.0	0.25	243	87	128	12
↓	↓	↓	↓	↓	↓	↓	.50	243	87	106	9
							.75	243	86	89	7
							1.00	244	86	77	6
					.2	.4	.25	241	107	126	-68
					↓	↓	.50	241	106	104	-75
							.75	241	106	88	-79
							1.00	242	106	75	-80
	.2	.8					.25	164	98	92	-106
	↓	↓					.50	164	98	77	-111
							.75	165	98	65	-114
							1.00	166	98	56	-115
.2							1.00	166	98	51	-115
5.0	↓	↓	↓	↓	↓	↓	1.00	166	98	82	-115

TABLE III.- EFFECTIVENESS OF SOLAR AND LUNAR RADIATION SHIELDS UPON THE TEMPERATURE OF A VEHICLE WITH INTERNALLY GENERATED HEAT AT THE SUBSOLAR POINT; ZERO SKIN CONDUCTANCE



Vehicle surface properties			Heat generated within the cylindrical section, watts	Vehicle temperatures, °F	
α_s/ϵ	α_s	ϵ		Conical section	Cylindrical section
1.0	1.0	1.0	2,500	56	-26
↓	↓	↓	5,000	57	29
↓	↓	↓	7,500	57	70
↓	↓	↓	10,000	57	102
.2	.16	.8	2,500	51	-14
↓	↓	↓	5,000	51	45
↓	↓	↓	7,500	51	89
↓	↓	↓	10,000	52	124
5.0	.5	.1	500	82	6
↓	↓	↓	1,000	82	71
↓	↓	↓	1,500	82	119
↓	↓	↓	2,000	82	158

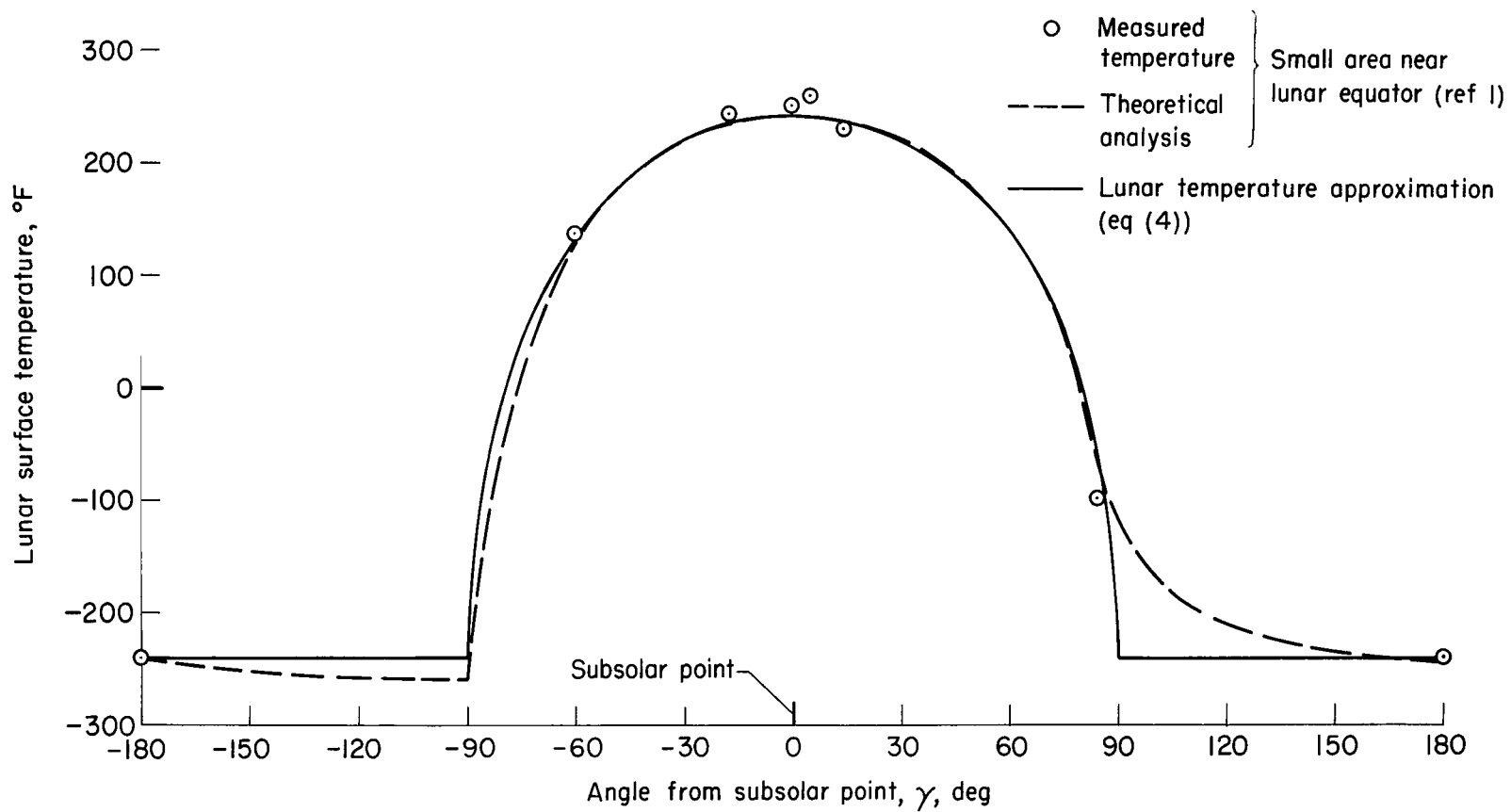


Figure 1.- Temperature variation of the lunar surface.

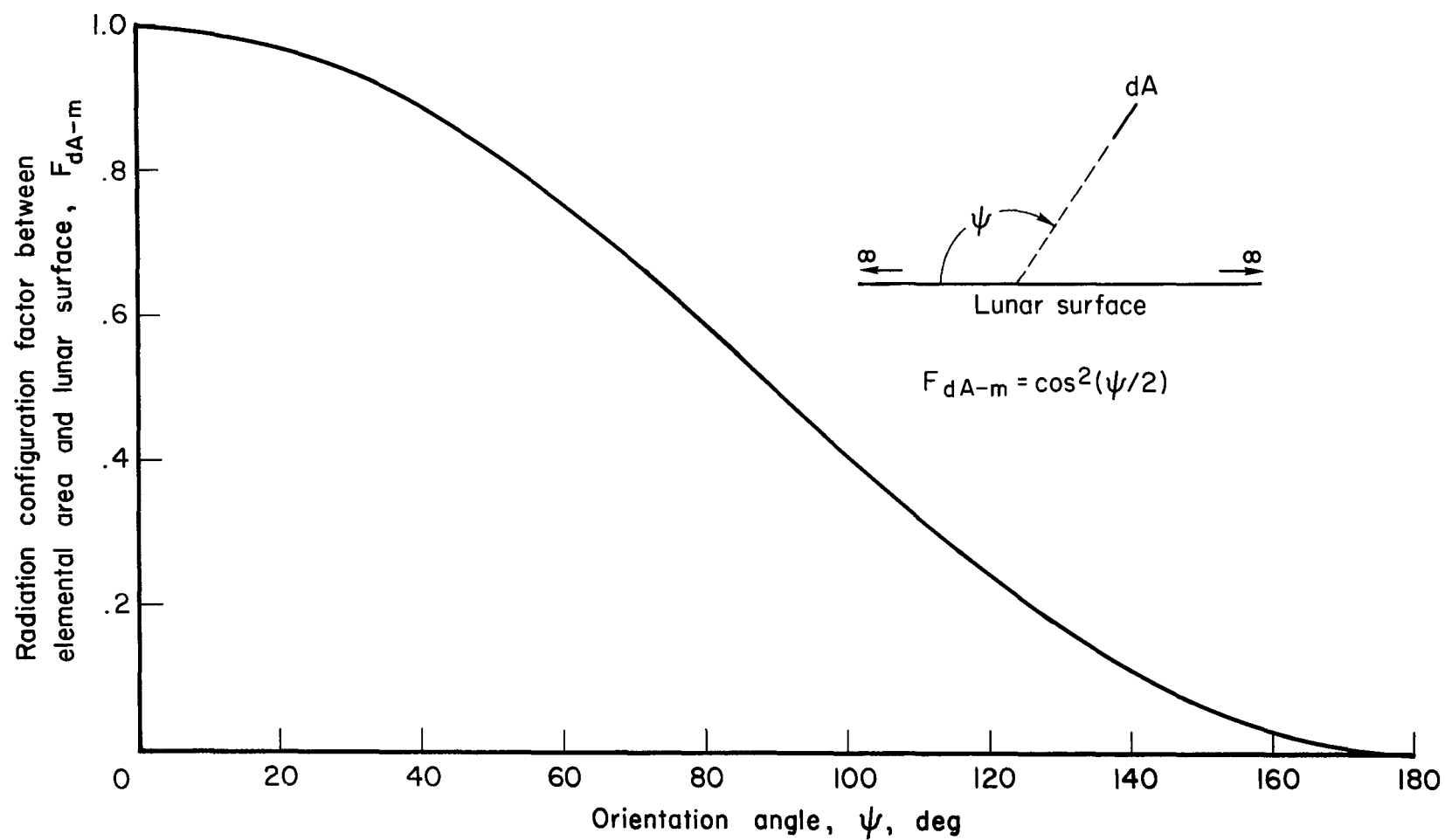


Figure 2.- Configuration factor for an elemental area inclined to an infinite plane.

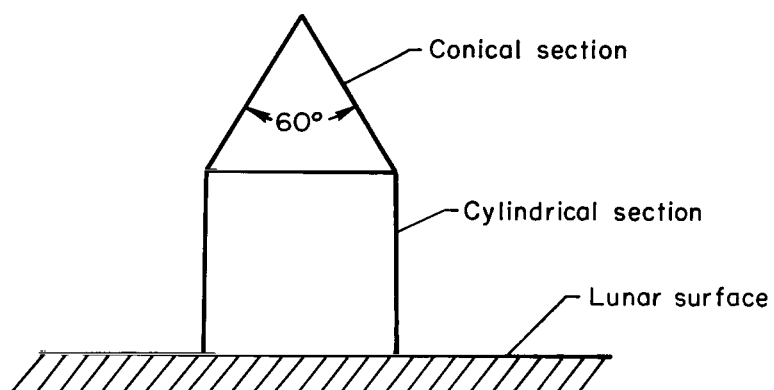
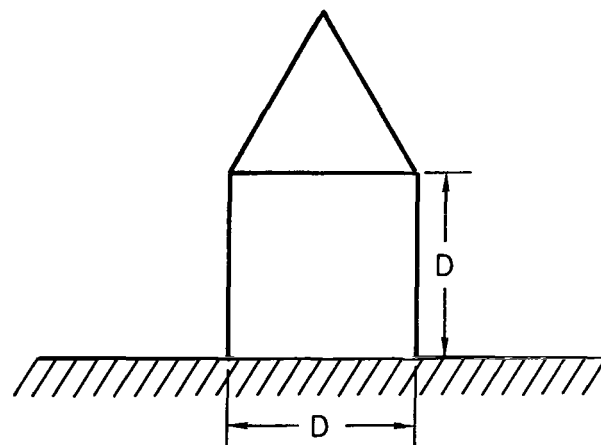
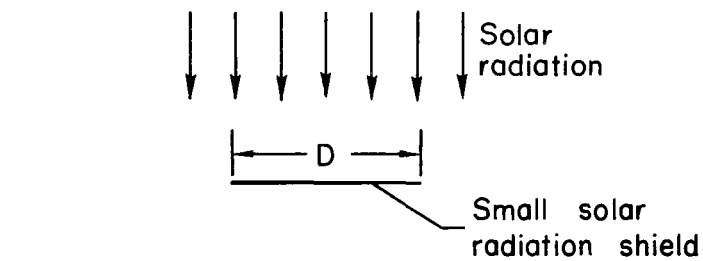
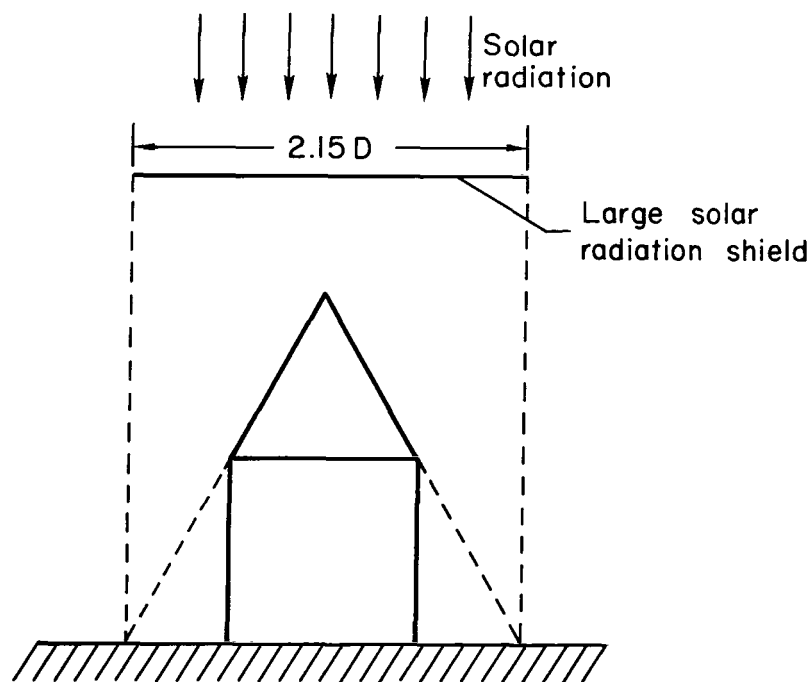


Figure 3.- Basic vehicle configuration.

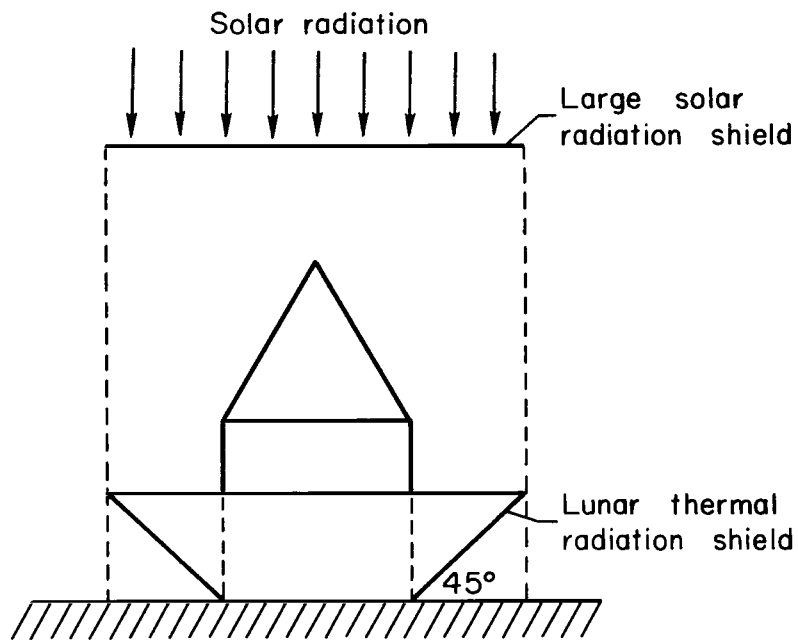


(a) Small solar shield.

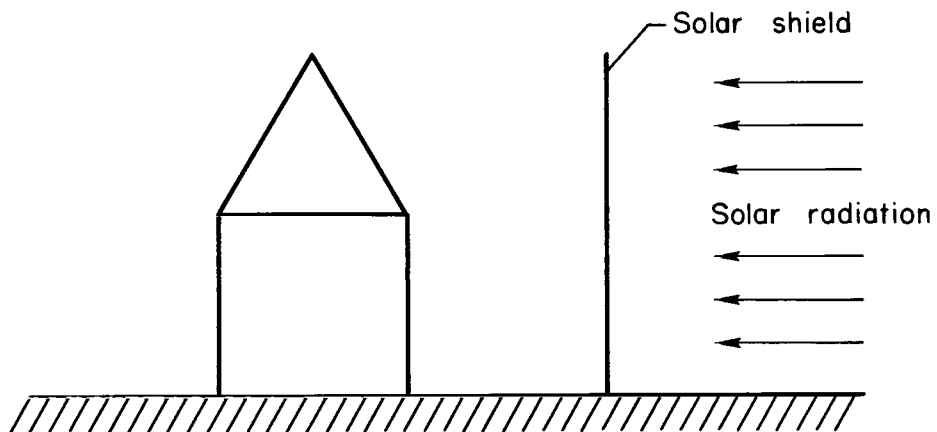


(b) Large solar shield.

Figure 4.- Shielded vehicle configurations.

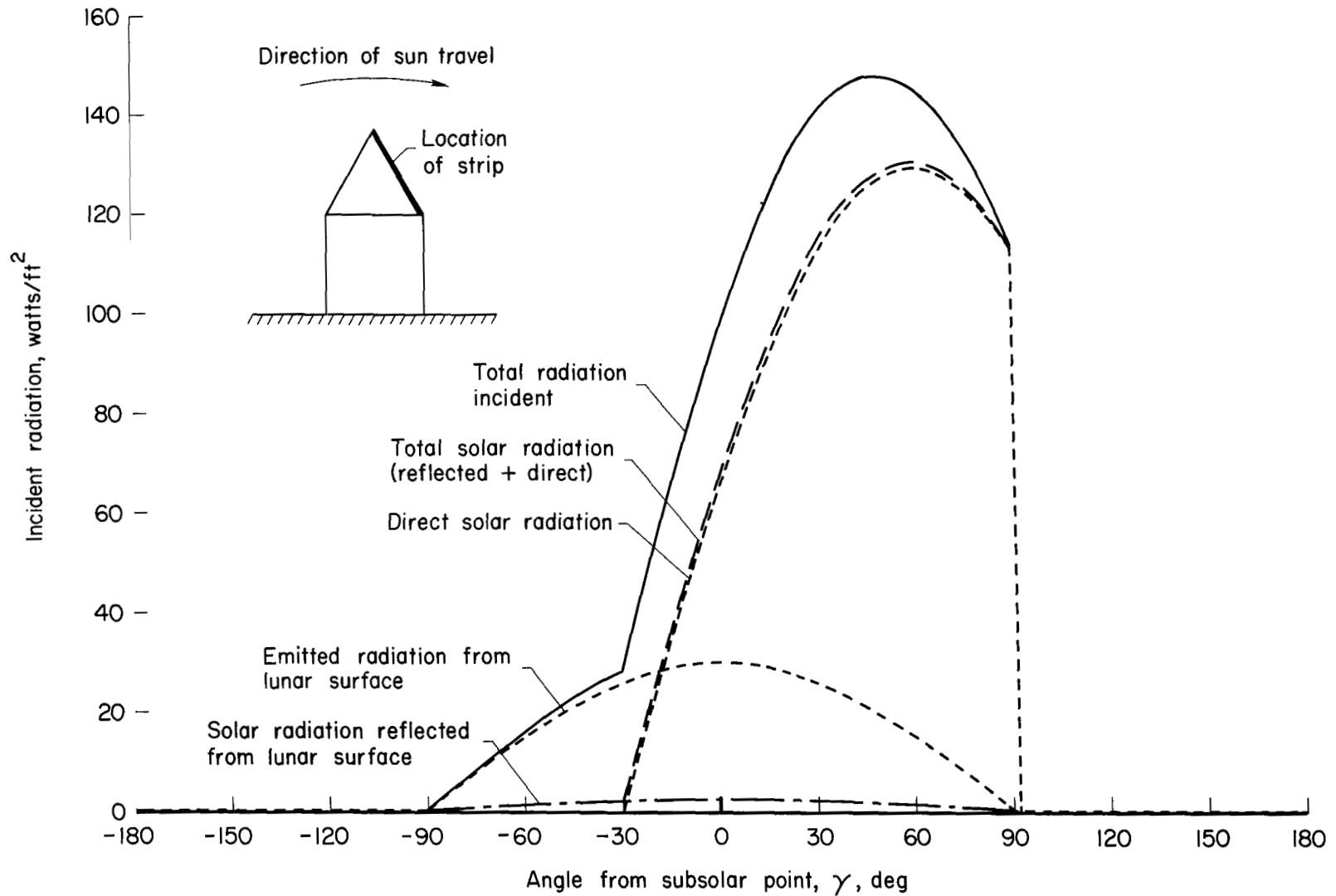


(c) Solar shield and lunar shield.



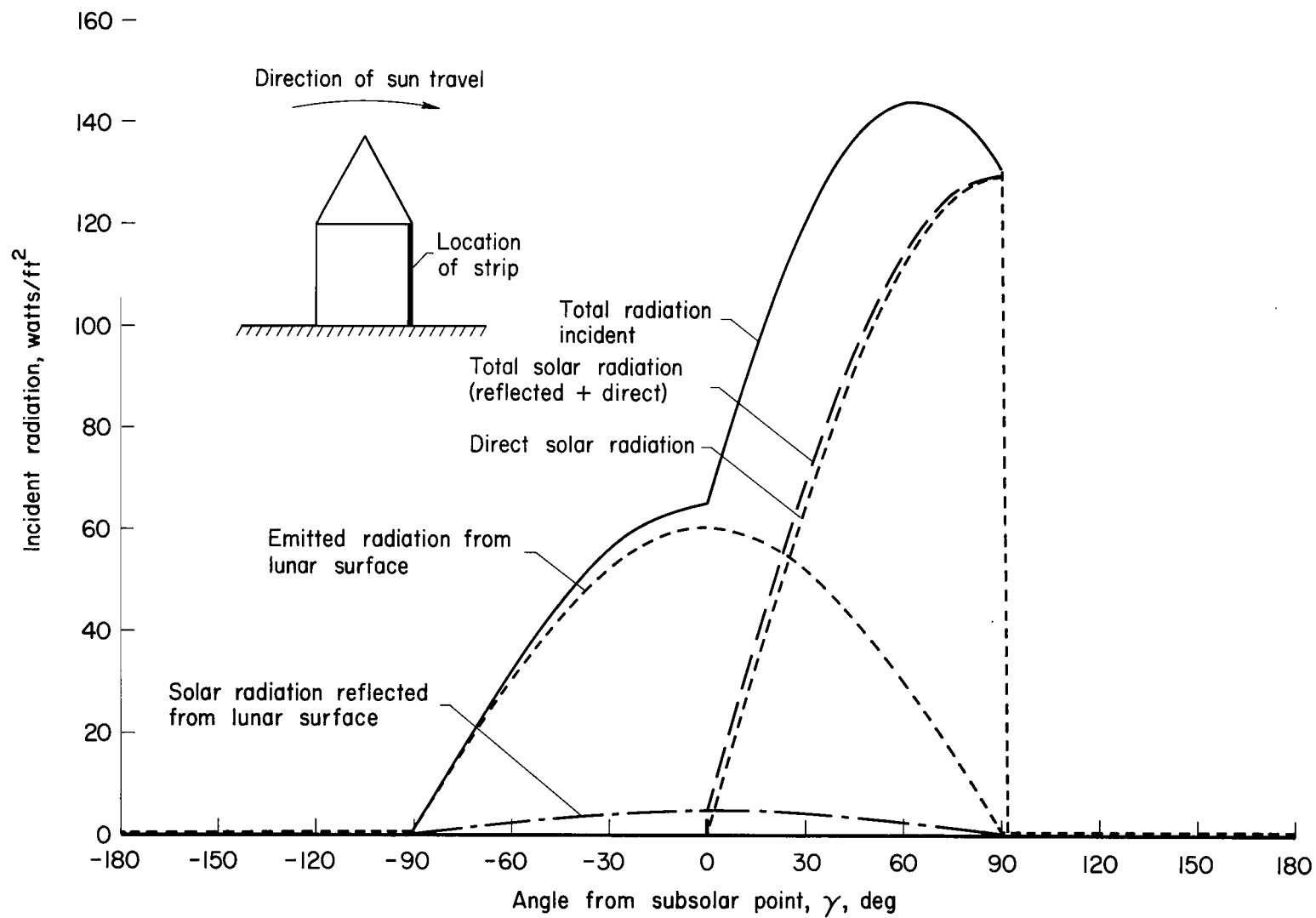
(d) Solar shield - side illumination.

Figure 4.- Concluded.



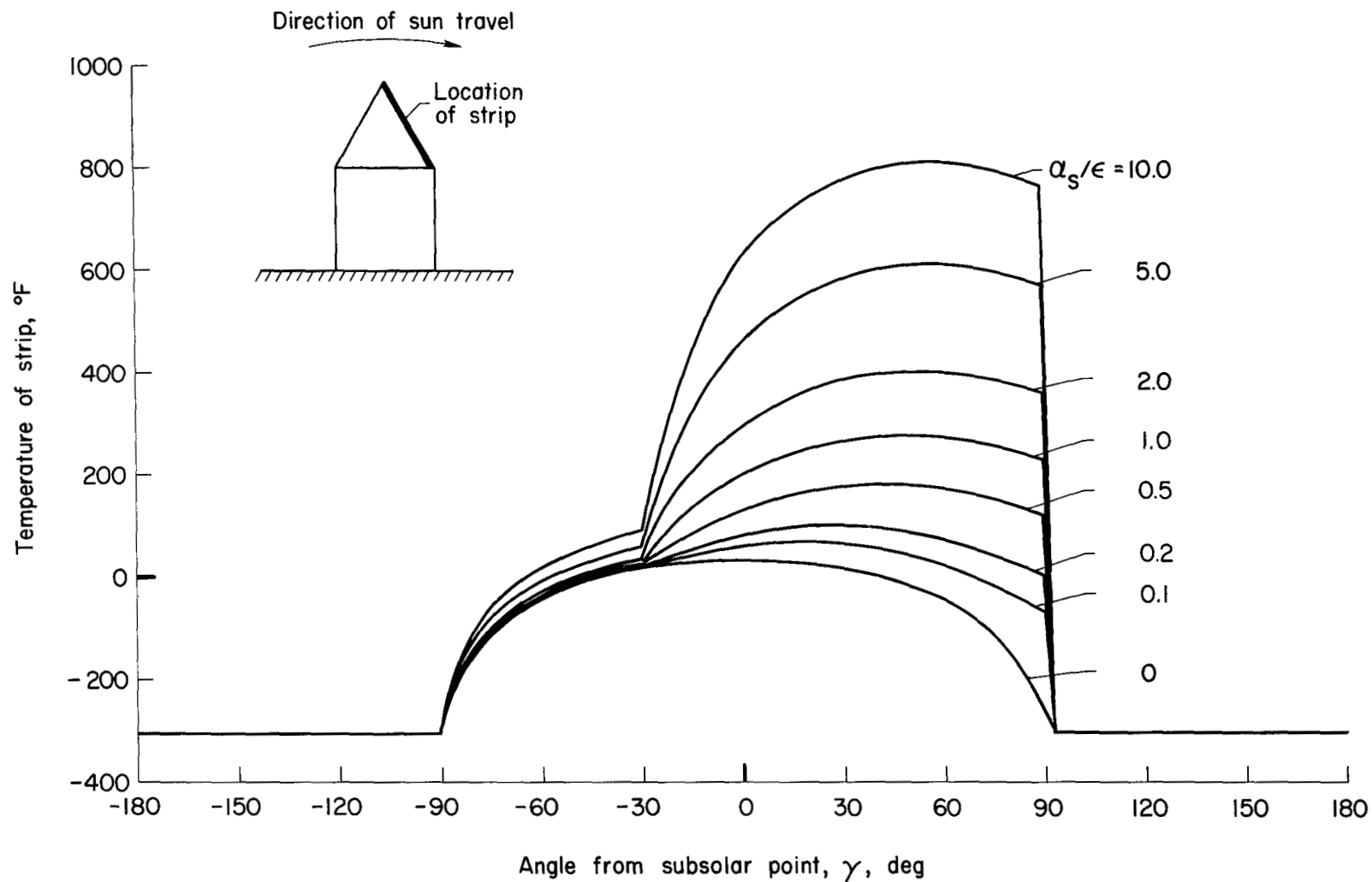
(a) Conical section.

Figure 5.- Incident radiation on a strip on the unshielded vehicle during a lunar day.



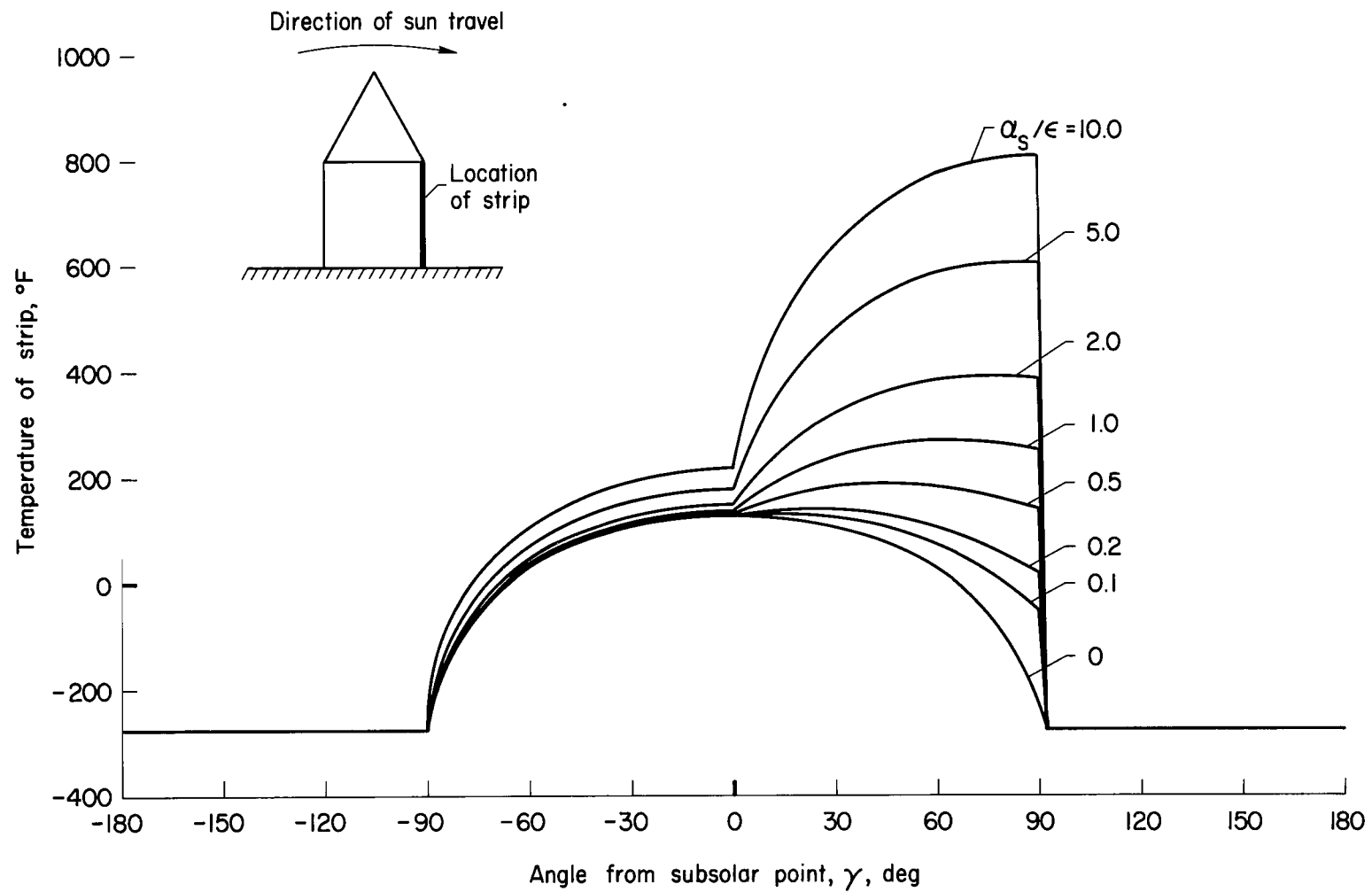
(b) Cylindrical section.

Figure 5.- Concluded.



(a) Conical section.

Figure 6.- Temperature variation of a strip on the unshielded vehicle during a lunar day; conductance and internal heat both zero.



(b) Cylindrical section.

Figure 6.- Concluded.

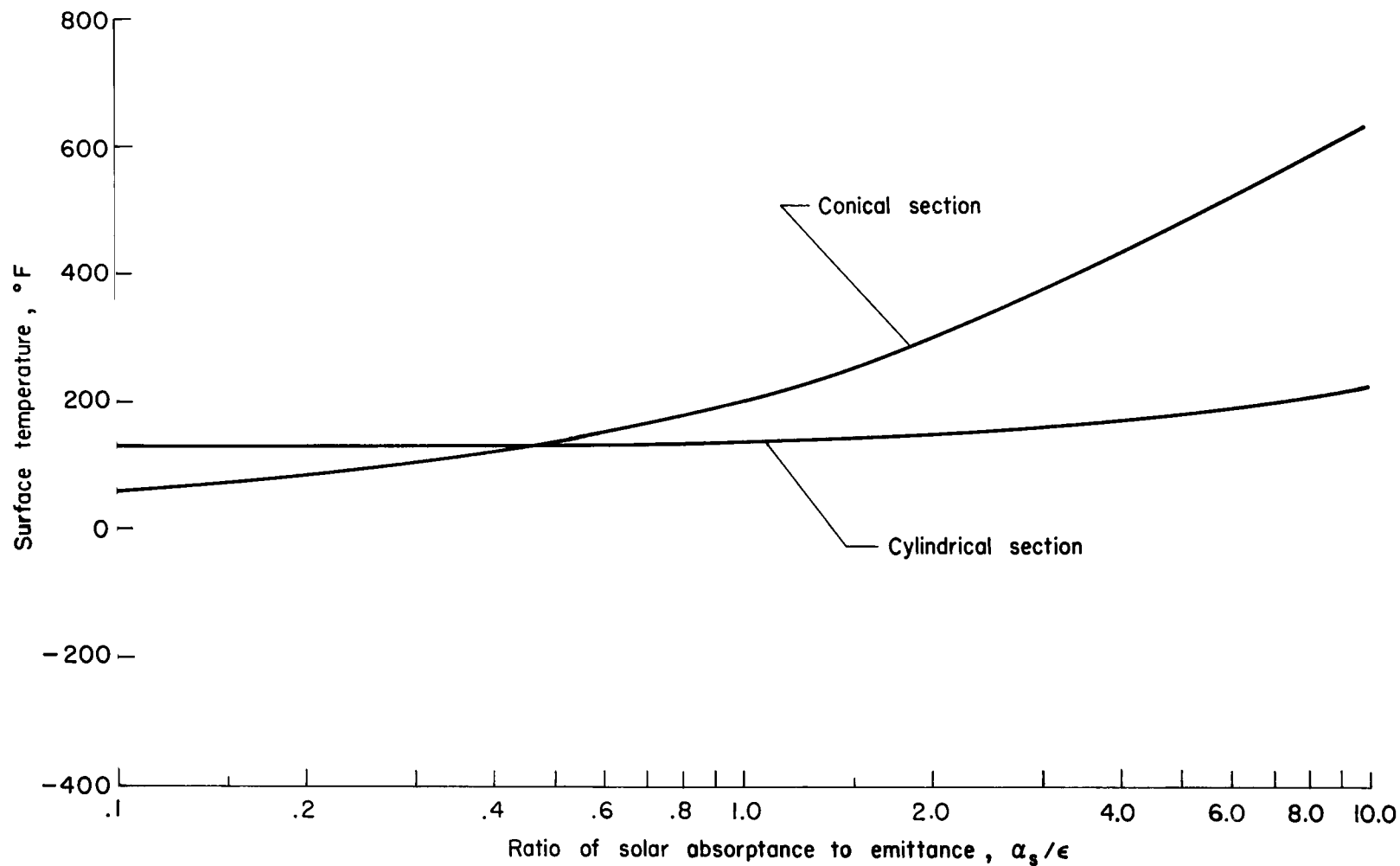


Figure 7.- Effect of the ratio of solar absorptance to emittance on the surface temperatures of the unshielded vehicle at the subsolar point; conductance and internal heat both zero.

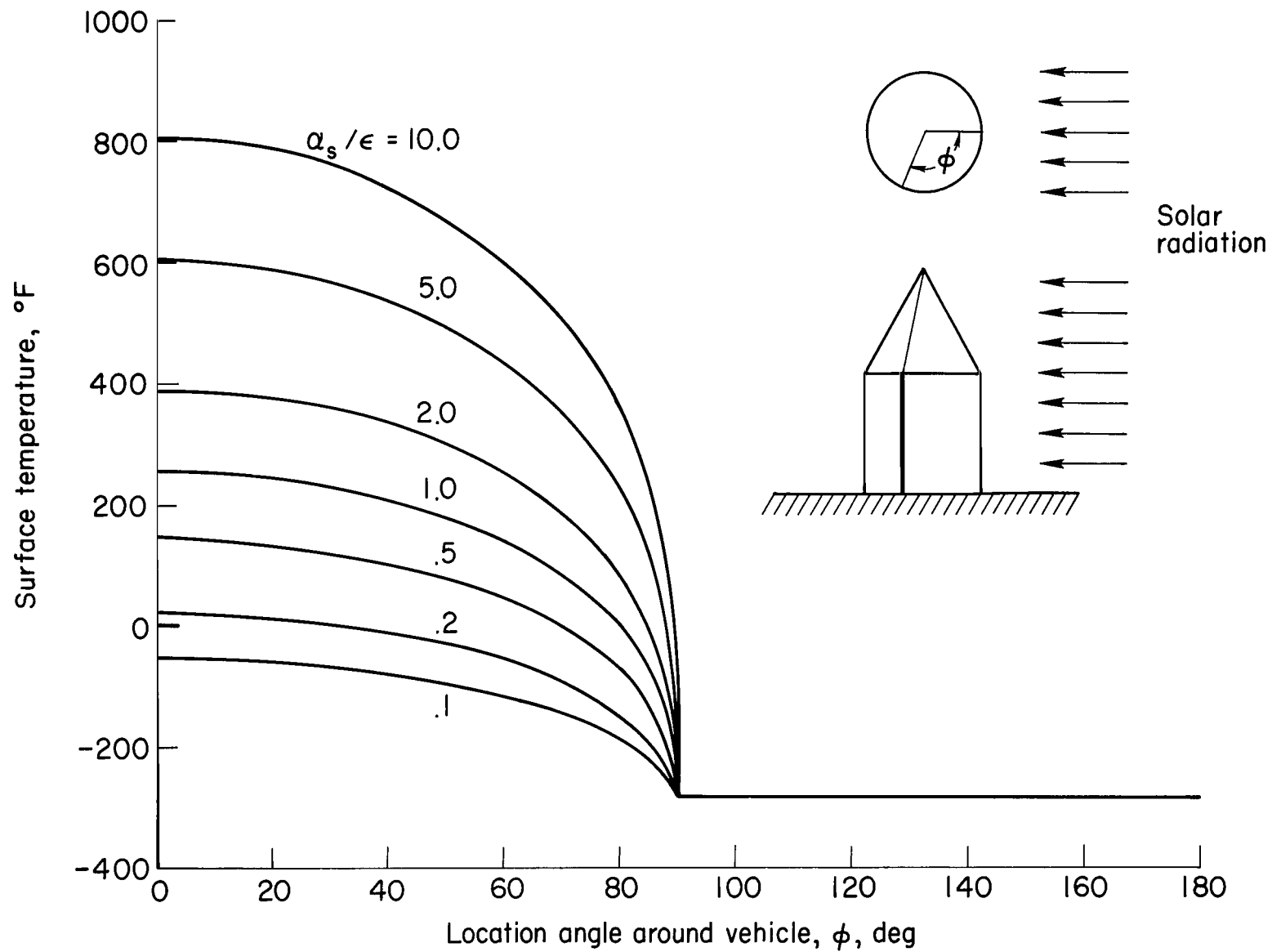
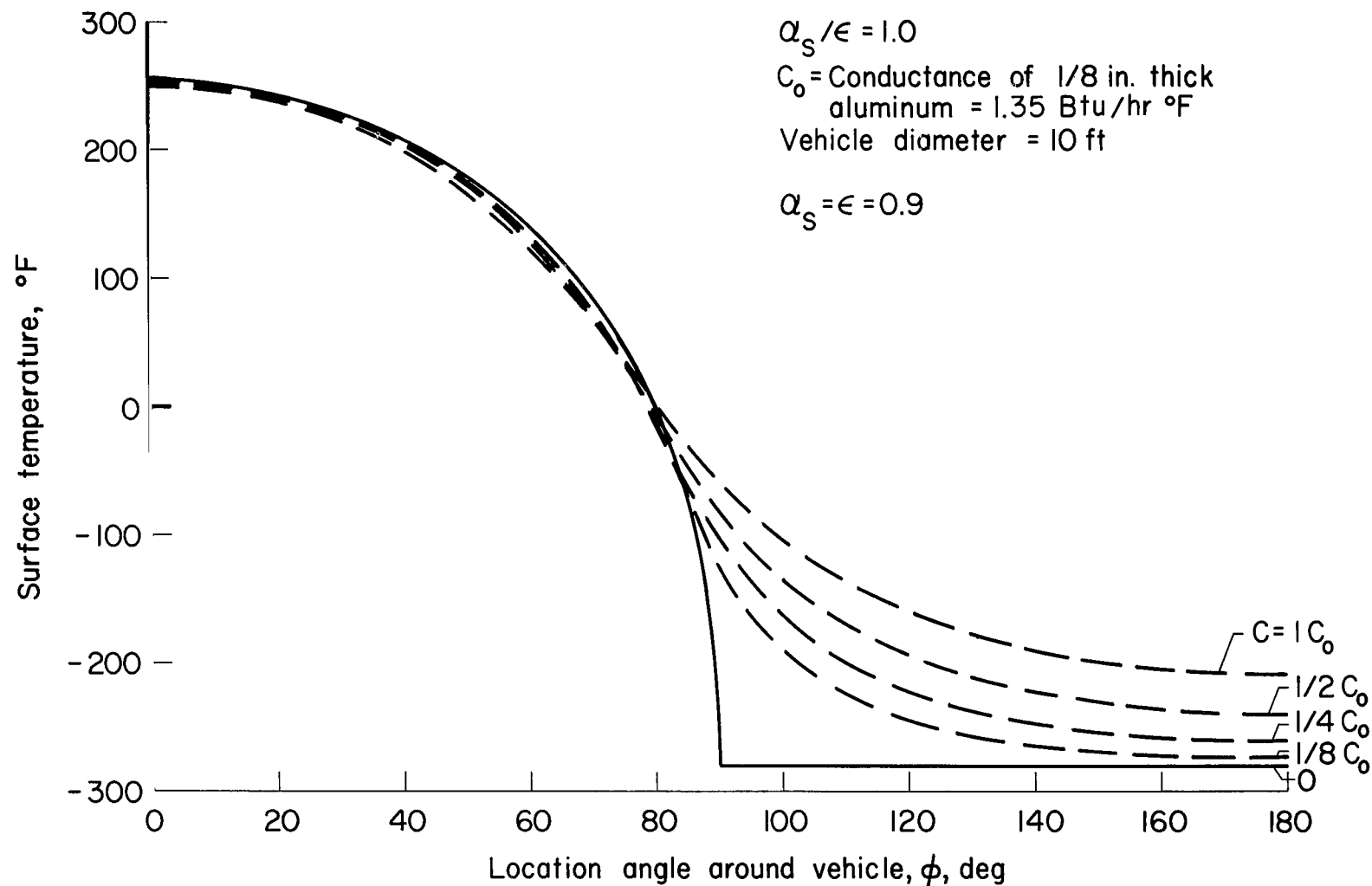
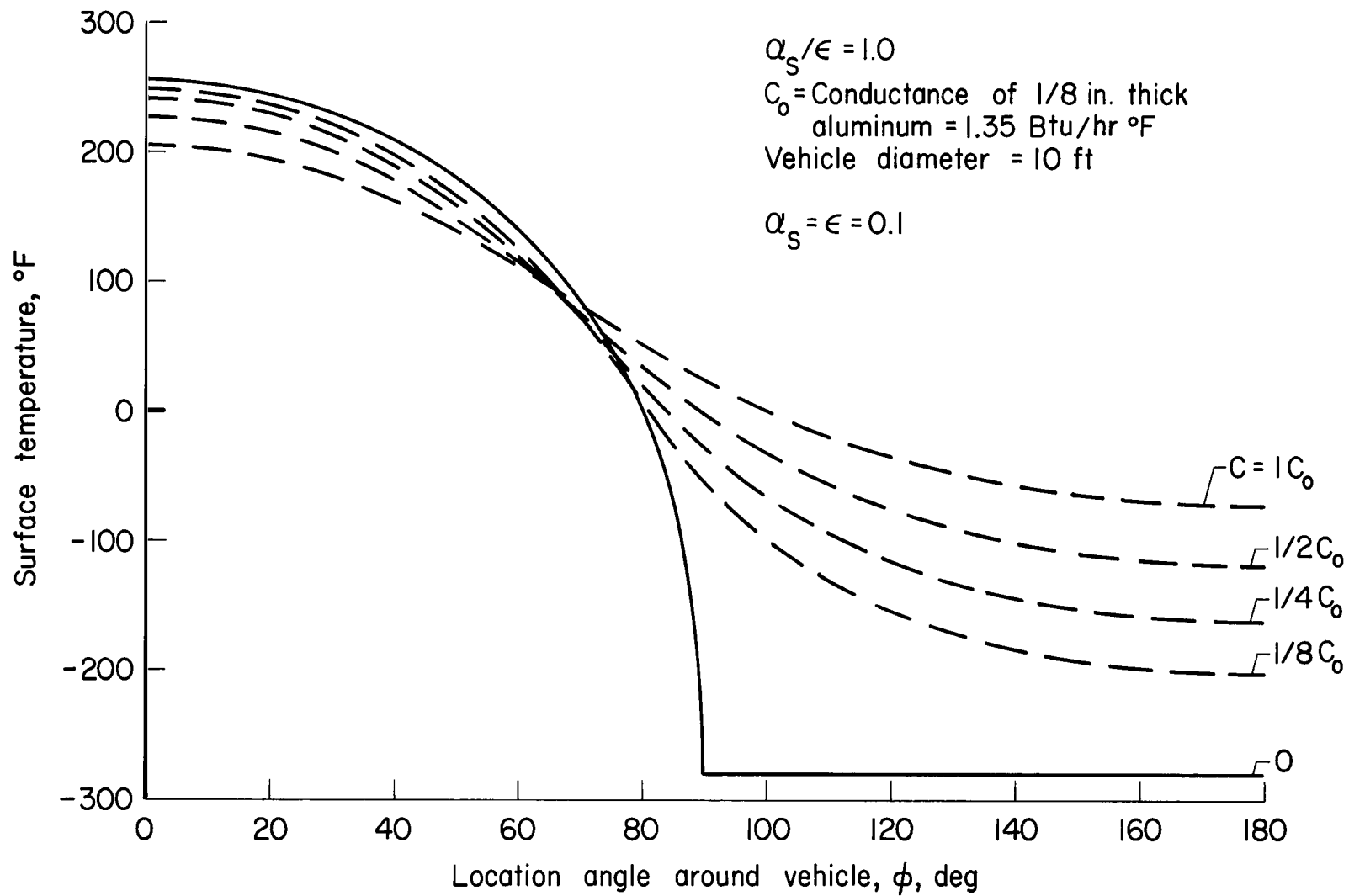


Figure 8.- Temperature variation around the cylindrical section of the unshielded vehicle when illuminated from the side; conductance and internal heat both zero.



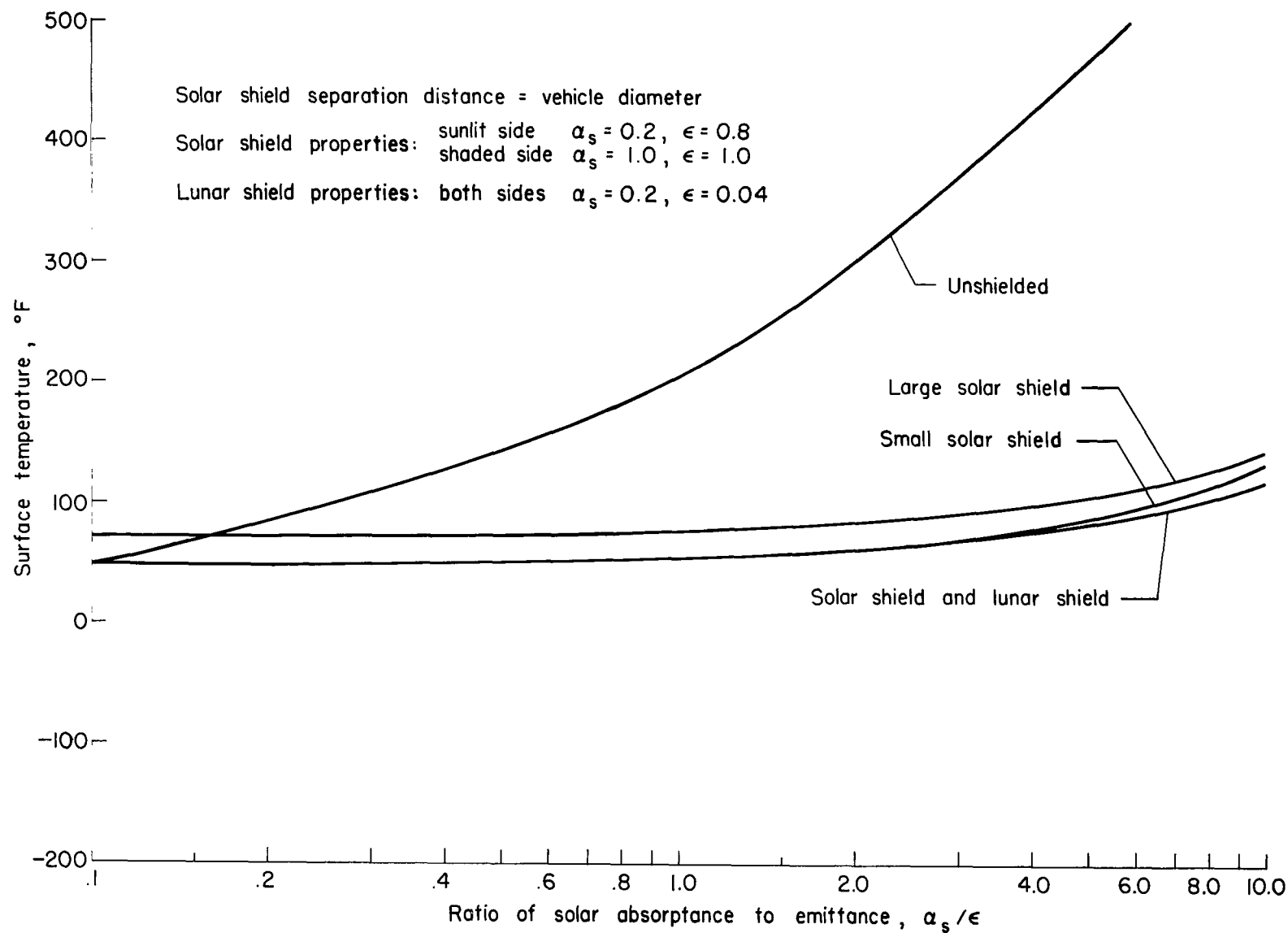
(a) High-emittance surface.

Figure 9.- Effect of thermal conductance upon the temperature variation around the cylindrical section of the vehicle when illuminated from the side; no internal heat.



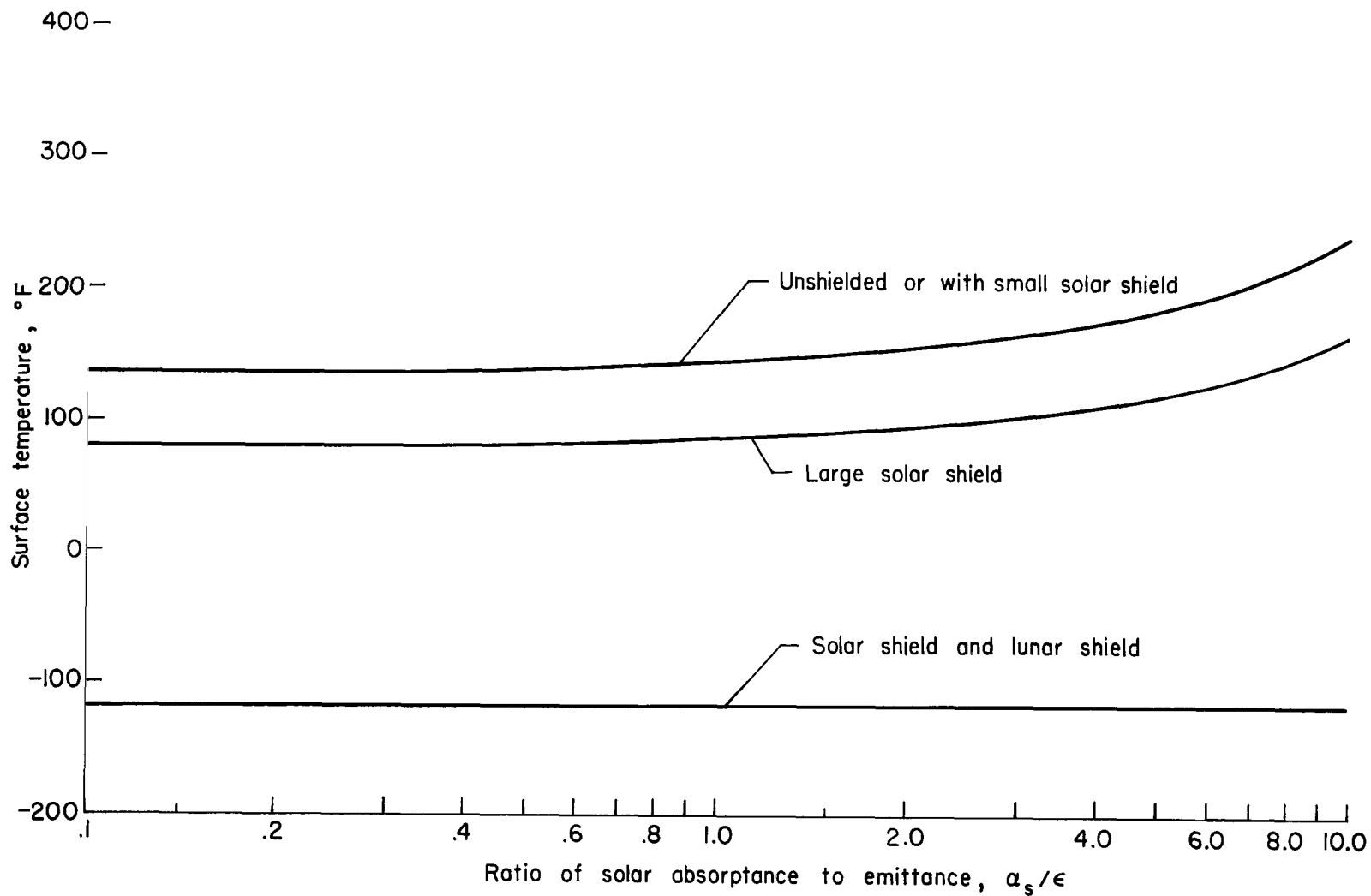
(b) Low-emittance surface.

Figure 9. - Concluded.



(a) Conical section.

Figure 10.- Effectiveness of solar and lunar radiation shields at the subsolar point as a function of the α_s/ϵ ratio on the vehicle; conductance and internal heat both zero.



(b) Cylindrical section.

Figure 10.- Concluded.

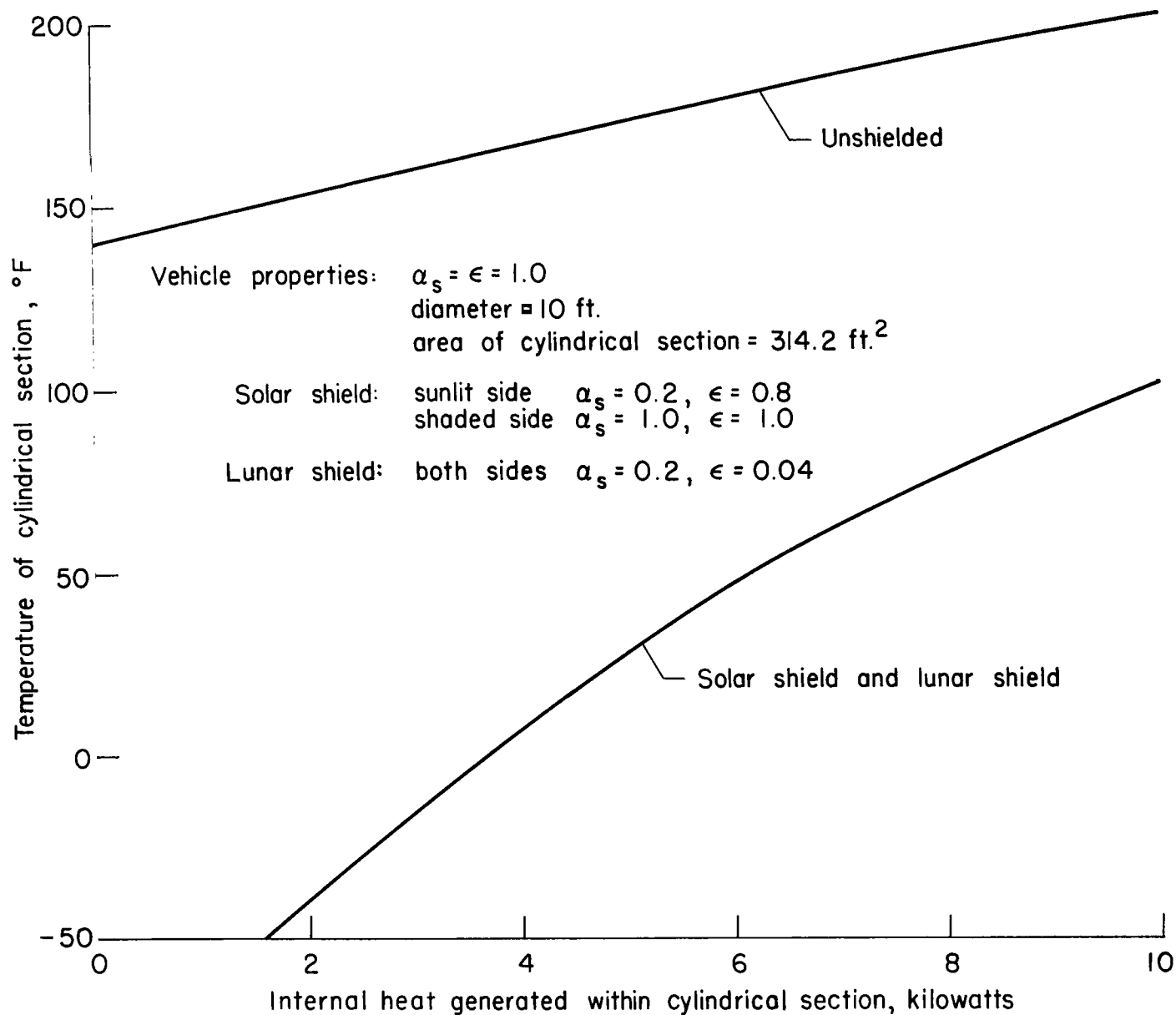


Figure 11.- Effectiveness of solar- and lunar-radiation shields upon the temperatures on a vehicle at the subsolar point with internally generated heat.

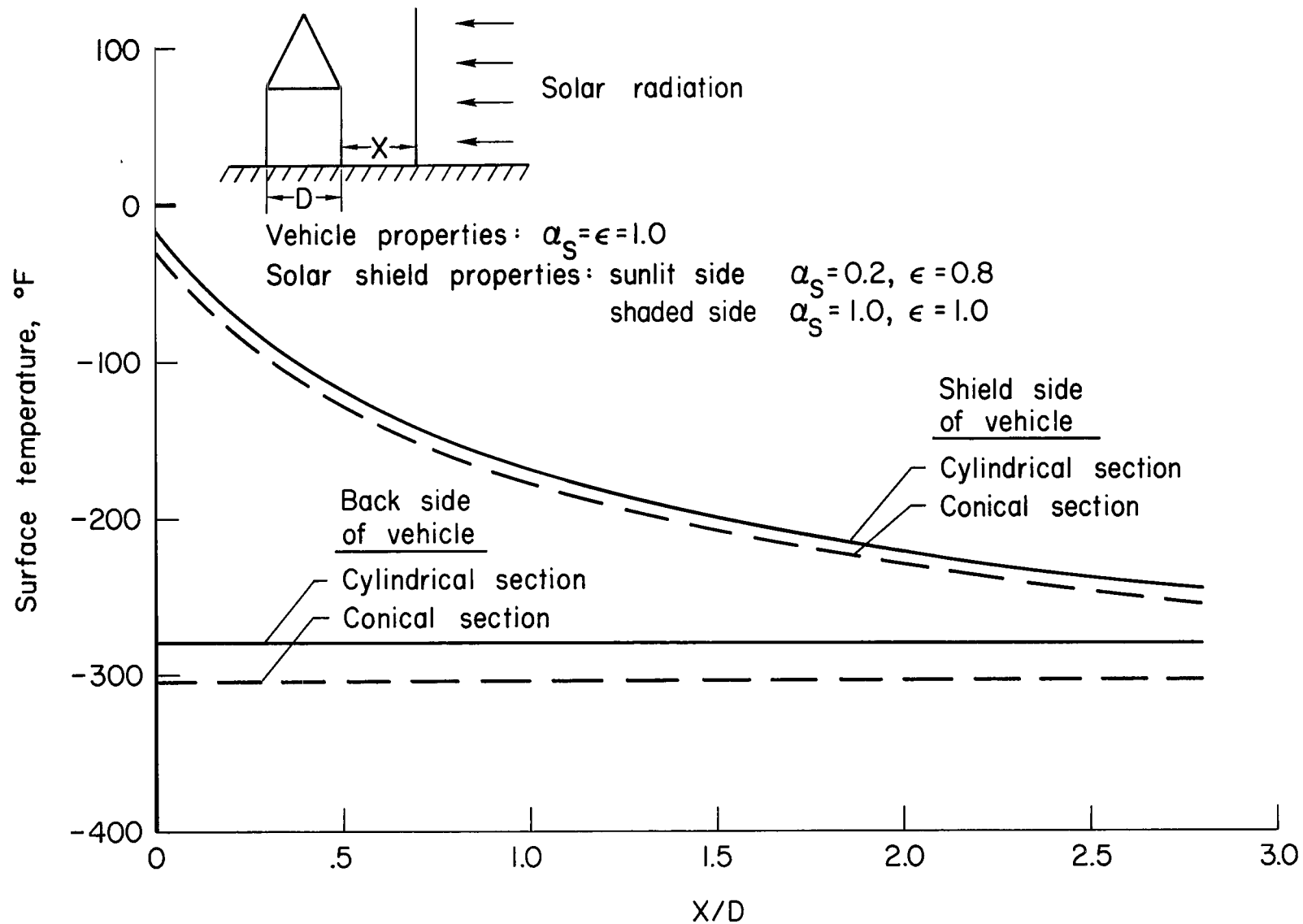
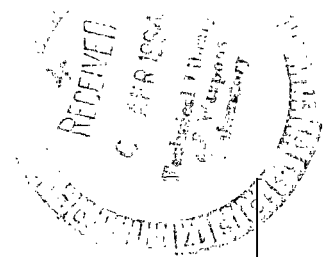


Figure 12.- Effectiveness of a solar-radiation shield when the vehicle is illuminated from the side; conductance and internal heat both zero.

2/17/81
omb
S



"The National Aeronautics and Space Administration . . . shall . . . provide for the widest practical appropriate dissemination of information concerning its activities and the results thereof . . . objectives being the expansion of human knowledge of phenomena in the atmosphere and space."

—NATIONAL AERONAUTICS AND SPACE ACT OF 1958

NASA SCIENTIFIC AND TECHNICAL PUBLICATIONS

TECHNICAL REPORTS: Scientific and technical information considered important, complete, and a lasting contribution to existing knowledge.

TECHNICAL NOTES: Information less broad in scope but nevertheless of importance as a contribution to existing knowledge.

TECHNICAL MEMORANDUMS: Information receiving limited distribution because of preliminary data, security classification, or other reasons.

CONTRACTOR REPORTS: Technical information generated in connection with a NASA contract or grant and released under NASA auspices.

TECHNICAL TRANSLATIONS: Information published in a foreign language considered to merit NASA distribution in English.

TECHNICAL REPRINTS: Information derived from NASA activities and initially published in the form of journal articles or meeting papers.

SPECIAL PUBLICATIONS: Information derived from or of value to NASA activities but not necessarily reporting the results of individual NASA-programmed scientific efforts. Publications include conference proceedings, monographs, data compilations, handbooks, sourcebooks, and special bibliographies.

Details on the availability of these publications may be obtained from:

SCIENTIFIC AND TECHNICAL INFORMATION DIVISION
NATIONAL AERONAUTICS AND SPACE ADMINISTRATION

Washington, D.C. 20546